

New massive X-ray binary candidates from the ROSAT Galactic Plane Survey*

I - Results from a cross-correlation with OB star catalogues

C. Motch^{1,2}, F. Haberl², K. Dennerl², M. Pakull¹, and E. Janot-Pacheco³

¹ Observatoire Astronomique, UA 1280 CNRS, 11 rue de l'Université, F-67000 Strasbourg, France

² Max-Planck-Institut für extraterrestrische Physik, D-85740 Garching bei München, Germany

³ Instituto Astronómico e Geofísico, Universidade de São Paulo, Caixa Postal 9638, 01065-970 São Paulo, Brazil

Accepted for publication in *Astronomy & Astrophysics Supplement Series*

Abstract. We report the discovery of several new OB/X-ray accreting binary candidates. These massive systems were found by cross-correlating in position SIMBAD OB star catalogues with the part of the ROSAT all-sky survey located at low galactic latitudes ($|b| \leq 20^\circ$) and selecting the early type stars which apparently displayed the most significant excess of X-ray emission over the 'normal' stellar level. The present search is restricted to stars earlier than B6 and X-ray luminosities $\geq 10^{31} \text{ erg s}^{-1}$. Follow-up optical and X-ray observations allowed to remove misidentified OB stars and spurious matches with interloper X-ray emitters (mostly active coronae) leaving five very likely new massive X-ray binaries: the O7 star LS 5039 and the Be stars BSD 24-491, LS 992, LS 1698 and LS I +61 235. This latter source was already mentioned in an earlier paper. LS 1698 is the probable optical counterpart of the hard X-ray transient 4U 1036-56.

These new candidates have 0.1-2.4 keV un-absorbed luminosities $\geq 2 \cdot 10^{33} \text{ erg s}^{-1}$ indicating an accreting neutron star or black hole. On the average their soft X-ray luminosities are comparable to those observed from hard X-ray transients in quiescence or from persistent low luminosity Be/X-ray sources. The four Be stars have Balmer emission slightly less intense than previously known systems showing strong outbursts. This suggests that the relative weakness of the circumstellar envelope may explain the low luminosities to some extent.

Two additional X-ray binary candidates, HD 161103 and SAO 49725 require further confirmation of their

Send offprint requests to: C. Motch

* Partly based on observations obtained at the Observatoire de Haute-Provence, CNRS, France, on observations collected at the European Southern Observatory La Silla, Chile, with the 2.2 m telescope of the Max-Planck-Society and on observations acquired at the Laboratorio Nacional de Astrofísica, CNPq, Brazil

X-ray excess. Their lower soft X-ray luminosities ($1-5 \cdot 10^{32} \text{ erg s}^{-1}$) could qualify them as Be + accreting white dwarf systems.

Four other B stars in the Orion and Canis Major OB associations, HD 38087, HD 38023, HD 36262 and HD 53339 exhibit X-ray flux excesses in the range $2-7 \cdot 10^{31} \text{ erg s}^{-1}$ whose origin is unclear. Finally very soft X-ray emission was detected from HR 2875 suggesting the presence of a non-accreting white dwarf companion to the B5 star.

Key words: X-ray: stars, Stars: early, Stars: emission-line, Be, neutron stars, white dwarfs

1. Introduction

Massive X-ray binaries were among the very first X-ray sources detected and optically identified more than 20 years ago. These systems consist of a compact object, a magnetized neutron star (X-ray pulsar) or a black hole, in orbit around a massive OB star. One usually distinguishes three subtypes depending on whether the X-ray source accretes matter through Roche lobe overflow via an accretion disc (e.g. LMC X-4), from the high velocity wind of an early type star (e.g. Vela X-1) or from a low velocity extended envelope around a Be star (e.g. A0535+26). Because Bondi-Hoyle accretion (Bondi & Hoyle 1944) is extremely sensitive to the relative velocity of the orbiting compact object with respect to the circumstellar material, the low velocities and high densities usually observed in Be envelopes provide rather favourable conditions for accretion and not surprisingly, the majority of the known massive X-ray binaries are in fact Be/X-ray systems (see

Van den Heuvel & Rappaport 1987 and Apparao 1994 for recent reviews).

Sporadic ejection of matter often observed in single Be stars combined with large variations of the accretion radius along the eccentric orbit explain the fact that most of these objects appear to be highly variable or even transient sources. The known massive X-ray binaries exhibit a large range of luminosities (10^{33-38} erg s $^{-1}$; 1-10 keV). In spite of their concentration at low galactic latitude, their hard X-ray spectra resulting from the accretion onto a highly magnetized young neutron star or in rare cases onto a black hole allows to detect them very deeply into the galactic plane especially during the outburst states. However, large interstellar absorption often renders optical identification very difficult.

As individual objects, their scientific importance is high since, for instance, a large fraction of our knowledge on the masses of neutron stars comes from the Doppler analysis of these X-ray pulsars. By studying the variation of the X-ray luminosity and absorption by the intervening medium along the orbit, i.e. by using the neutron star as a probe of the stellar environment, several characteristics of the circumstellar envelopes (e.g. Waters et al. 1989; Motch et al. 1991a) or of the stellar wind (e.g. Haberl et al. 1989, Haberl & White 1990) can be constrained.

As a class of objects, their scientific importance is also large since they could account for part, if not all, of the hard diffuse emission observed in our Galaxy (e.g. the hard X-ray ridge emission; Warwick et al. 1985) and more generally in starburst galaxies (e.g. Griffiths & Padovani 1990) where they may turn on as bright X-ray sources already $9 \cdot 10^6$ yr after the onset of star formation. Finally, these binaries may end their evolution by forming high mass binary pulsars (see e.g. Verbunt & van den Heuvel, 1995 for a review).

With a 1-10 keV sensitivity of the order of $2.5 \cdot 10^{-11}$ erg cm $^{-2}$ s $^{-1}$, X-ray surveys carried out before ROSAT had detection threshold luminosities of $L_X \approx 3 \cdot 10^{33}$ (d/1 kpc) 2 ergs $^{-1}$. Therefore, many high mass systems may still remain hidden in the galactic plane, especially those powered by high velocity wind accretion and those belonging to the low end of the Be/X-ray luminosity function. Although the low energy range of the ROSAT PSPC may not be the best suited for searching such objects in regions of high interstellar absorption, the ROSAT all-sky survey has nevertheless the capability to detect these systems up to distances 10 times larger than previous experiments in directions relatively clear of interstellar absorption.

In this paper we present the result of a search for new OB/X-ray systems using the cross-correlation in position of all O and B stars listed in the SIMBAD database with the source list of the ROSAT galactic plane survey (RGPS; Motch et al. 1991b). By definition the RGPS is the part of the ROSAT all-sky survey (RASS; Voges 1992) restricted to regions of absolute galactic latitudes below 20° . The

ROSAT satellite and instrumentations are described in Trümper (1983) and Pfeffermann et al. (1986).

This work extends the preliminary search carried out by Meurs et al. (1992) for a subsample of early type stars. By selecting stars which apparently exhibited a L_X/L_{bol} ratio in excess of what is expected from normal stellar OB X-ray emission we could isolate a subset of candidate objects. Follow-up optical and pointed ROSAT observations allowed to assess the reality of the X-ray luminosity excess and resulted in the probable discovery of five new massive X-ray binaries with an additional two likely candidates.

In section 2 we present the methods and results of the initial selection using SIMBAD entries and the ROSAT survey source list. In sections 3 to 5 we analyze our optical and X-ray survey and pointed ROSAT observations and draw conclusions on the reality of each new candidate massive X-ray binary. We then discuss the nature of the new systems discovered and their relation to the already known population of massive X-ray binaries. A preliminary report on this work was given in Motch et al. (1996c,d).

2. Cross-correlation of the ROSAT all-sky survey source list with SIMBAD OB stars

2.1. The ROSAT source list

The source list considered here arises from the first ROSAT all-sky survey data reduction as completed by 1991 October by the Scientific Analysis System Software (SASS; Voges et al. 1992). This software provides for each source the position, count rates and hardness ratios HR1 and HR2 defined as

$$\begin{aligned} \text{HR1} &= \frac{(0.40 - 2.40) - (0.07 - 0.40)}{(0.07 - 2.40)} \\ \text{HR2} &= \frac{(1.00 - 2.40) - (0.40 - 1.00)}{(0.40 - 2.40)} \end{aligned}$$

where (A-B) is the raw count rate in the energy range A to B in keV. Because of spacecraft problems no data were available for about 5% of the sky located between ecliptic longitudes 41° and 49° and ecliptic longitudes 221° and 229° . The accumulation by 2° wide strips along the great scan circles yields variations of sensitivity perpendicular to the strip and overlapping at high ecliptic latitudes may produce multiple detection of the same source in adjacent strips. The lists of sources derived from each strip were then merged into a single master list totaling about 15,000 sources at $|b| \leq 20^\circ$. The merging process assumed that a source detected in two or more strips was the same when the difference in position was less than a minimum value of one survey sky pixel ($90''$) or less than the combined positional errors. The strip oriented analysis does not allow an easy estimate of the sensitivity of detection in a given part of the sky but allows quick detection.

The errors on ROSAT X-ray positions have two different origins. First, the statistical uncertainty with which the centroid of the X-ray image is positioned on the pixel grid by the Maximum Likelihood source detection algorithm. Second, the systematic error in the knowledge of the satellite attitude for each photon collected in scan mode. The analysis of the subsample of the 13 known high mass X-ray binaries (HMXBs) detected in the RGPS by the SASS (see section 2.2 and Table 10), led to the conclusion that the systematic attitude error Δ_{att} to apply to survey positions was $\approx 8''$ and that the 95% confidence radius could be expressed as

$$r_{95} = 2.5 \times \sqrt{\Delta_{xy}^2 + \Delta_{att}^2}$$

where Δ_{xy} is the Maximum Likelihood error.

2.2. The SIMBAD database

The master list used for the cross-correlation was extracted from the SIMBAD database in 1990 and not later updated. SIMBAD early type stars are mostly recognized from HD, CD, BD, HR and SAO spectral information and associated literature. We list in Table 1 the distribution in spectral types of the SIMBAD stars located within 20° from the galactic plane, subdwarfs excluded. Stars having general spectral types 'OB' mostly originate from the Luminous Star (LS) catalogues compiled by the Hamburger Sternwarte and Warner and Swasey Observatories for both hemispheres (Hardorp et al. 1959, Stephenson & Sanduleak 1971). Another important group of 'OB' stars without precise spectral classification arises from the Vatican Emission line Star (VES) catalogue (McConnell & Coyne 1983). Most of the stars classified as 'OB' are in fact earlier than B3 (Slettebak & Stock 1957). Because of the heterogeneousness of the various OB catalogues, it is difficult to quantify with accuracy the completeness in magnitude of our input sample. The Luminous Star catalogue which gathers most of the faintest early type stars is apparently complete down to $B \approx 12$ over the whole galactic plane.

Table 1. Distribution in spectral types of the OB SIMBAD stars ($|b| \leq 20^\circ$)

Types	Number
O	702
B0 - B5	8016
B6 - B9	20194
'OB'	7177

We first extracted all SIMBAD entries which had an associated error circle overlapping a $3'$ wide box centered on each ROSAT source. This rather large search area allows the correlation of candidate OB/X-ray sources with objects having inaccurate coordinates such as some variable stars, or with supernova remnants. In a second step

we selected from the main correlation list all sources having a match within $1'$ with a star of spectral type O or B, retaining for each selected OB/X-ray association the entire list of possible candidates extracted in the $3'$ wide box. The restriction on angular distance allows to eliminate many spurious OB/X-ray matches since the 90% confidence ROSAT radius is usually less than $30\text{--}40''$ (Voges et al. 1992, corresponding to a 95% confidence radius in the range of $35\text{--}46''$) and optical positions of OB stars are known to better than $\approx 10''$. Thirteen sources which were thought to have a likelier identification than the proposed OB star were removed by hand from the correlation list (see Table 2). This happened for instance when a known active corona (RS CVn binary, pre-main sequence star) or a supernova remnant was also present in the ROSAT error circle. Pre-main sequence stars and RS CVn binaries are known to be sometimes bright soft X-ray sources with luminosities up to $10^{31} \text{ erg s}^{-1}$ (e.g. Montmerle et al. 1983, Walter & Bowyer 1981). Keeping in mind that our aim was to select only promising accreting candidates leaving doubtful identifications for a later study we decided to ignore these cases for the moment. On similar grounds, compact OB associations (i.e. groups of OB stars located within few arcminutes and appearing blended at the X-ray spatial resolution of the RASS) were not considered in this analysis because of the difficulty in assessing an individual X-ray to bolometric luminosity ratio for such objects. The B2V star HD 63177 ($V = 8.31$) tentatively associated with RX J0744.9-5257 was also taken off from the final correlation list since optical follow-up observations have shown the presence of a cataclysmic variable $\approx 40''$ away from the candidate B star (Motch et al. 1996a).

Finally, for the sake of comparison, we keep aside the group of 13 known massive X-ray binaries detected during the ROSAT all-sky survey at $|b| \leq 20^\circ$ (see Table 10). Of these, 9 were listed in the OB SIMBAD catalogues and retrieved correctly during the above selection process while 4 were added using data extracted from the literature (He 3-640, Cen X-3, 1H1909+096, EXO 2030+375). The final list of OB/ROSAT source associations contained a total of 237 sources entries split as shown in Table 3.

Table 3. The final OB/RGPS correlation list

Types	limiting radius	Number of X/OB associations
Known HMXBs	1 arcmin	13
All types	1 arcmin	224
O-B5 + 'OB'	1 arcmin	128
O-B5 + 'OB'	r_{95}	108
B6-B9	1 arcmin	96
B6-B9	r_{95}	79

Table 2. List of OB/X-ray associations removed from the main correlation list on the basis of the existence of a possible alternative identification. Count rates are taken from the SASS analysis of the survey and the optical information listed is entirely extracted from SIMBAD as in 1990

ROSAT Source name	count rate (10^{-3}s^{-1})	Proposed Identification	do _x (")	OB match	do _x (")		
		Name	Sp. type	Name	Sp. type		
RX J1022.2-5816	99±47	HD 90074	G6III	21	HD 302780	B9V	58
RX J2210.9+6323	27±14	ADS 15712 C		8	HD 210808	B5	32
RX J2101.6+6809	49±12	HZ Cep	Flare star	24	HD 200775	B2Ve	23
RX J2329.8+5833	49±19	HD 221237	A1V	52	ADS 16795G	B3	54
		+ADS 16795H/F ?					
RX J1520.2-3822	150±24	CD-37 10147C/D/B		11	HD 136125	B9V	46
RX J0344.5+3208	166±25	LkHA 95	PMS	59	HD 281159	B5V	57
RX J0345.6+3226	40±14	LkHA 329	K5IV-Ve	45	HD 281157	B5	22
RX J1544.3-4149	116±22	HR 5846	A0V	19	HD 140285B	B	24
RX J1612.2-2825	260±45	ADS 9953 B	F2V	32	HR 6029	B9V	8
RX J0510.3+3547	57±24	HP Aur ¹⁾	G0 (RS CVn)	2	HD 280603	B	25
RX J0535.9-0616	90±22	V1178 Ori		6	HD 37131	B9V	14
RX J1811.5-1925	680±70	SNR 011.2-00.3	SNR	15	LS 4738	B	16
RX J1158.3-5759	50±27	HD 104010 (+B)	G7+K0	15.5	HD 103996	B4V	8

¹⁾ The latest version of SIMBAD merges these two objects as a single RS CVn binary

2.3. The L_X/L_{bol} diagnosis for OB stars

All stars of spectral type earlier than \approx B5 emit soft X-rays (0.2-4.0 keV) with a roughly constant X-ray to bolometric luminosity ratio independent of the luminosity class and age (e.g. Long & White 1980; Pallavicini et al. 1981). Sciortino et al. (1990) show that the mean value of L_X/L_{bol} for O stars is close to $10^{-6.46}$ with about 10% of these early type stars having L_X/L_{bol} in the range of 10^{-6} - $10^{-5.5}$. From ROSAT survey data Meurs et al. (1992) find a mean $\log(L_X/L_{bol})$ of -6.8 ± 0.5 for 43 O3 to B2.5 stars with no strong difference between OB and OBe stars. Using ROSAT PSPC pointed observations, Cassinelli et al. (1994) find that the L_X/L_{bol} ratio decreases sharply with spectral types later than B1 and could reach $\approx 10^{-9}$ at B3V.

The physical origin of the X-ray emission is still a matter of debate. Several authors assumed a picture stretched from the solar case in which a hot corona located close to the stellar surface lies below the cooler, high speed velocity wind (see e.g. Cassinelli et al. 1981, Waldron 1984). Alternatively, Lucy & White (1980) proposed that blobs of high density formed in the expanding wind may produce shocks and consequently X-rays.

2.4. Computation of the X-ray to bolometric luminosity ratio

Interstellar extinction may alter quite significantly the ratio of X-ray to optical flux measured from these stars. Depending on the softness of the assumed intrinsic X-ray spectrum the decrease of the 0.1-2.4 keV PSPC count rate with increasing interstellar column density may be quicker or slower than that of the optical flux. For instance, the overall PSPC count rate produced by a T =

10^6 K thin thermal spectrum (Raymond & Smith 1977) will be steeply decreasing with column density and at N_H = 10^{21} cm⁻² it will be \approx 100 times more dimmed than any optical flux crossing the same interstellar medium. On the opposite, the PSPC count rate resulting from a power law energy distribution with a photon index of 1, typical for Be/X-ray systems, will decrease less rapidly with N_H than optical radiation.

In order to correct for interstellar extinction we computed the colour excess E(B-V) from the spectral types and magnitudes listed in SIMBAD. Intrinsic B-V were taken from Johnson (1966) and absolute magnitude and bolometric corrections are from Deutschman et al. (1976) and Humphreys & McElroy (1984). The corresponding column density was then used to compute the PSPC count rate to un-absorbed flux conversion factor assuming a 10^7 K thin thermal spectrum (e.g. Pallavicini et al. 1981). Finally, the X-ray luminosity was estimated using the distance derived from the colour excess and spectral type together with the catalogue V or B magnitudes.

Obviously, there exist several possible temperatures for normal OB X-ray emission. Chlebowski, Harnden & Sciortino (1989) find temperatures in the range of 3 to $9 \cdot 10^6$ K from Einstein data and Cassinelli et al. (1994) reach similar conclusions from ROSAT observations. By intentionally assuming a temperature on the hot side of the distribution we avoid a systematic overestimation of the X-ray luminosity when correcting for interstellar absorption. Only in the rare case of a soft component (e.g. $2 \cdot 10^6$ K) seen at very low N_H do we expect overestimation of the un-absorbed X-ray emission. If the intrinsic spectrum is actually described by a power law distribution of photon index 1-2 as expected for young accreting neutron stars (e.g. White et al. 1983) the effect on the un-

absorbed luminosities is not large since we overestimate them by at most a factor of 2 at low N_{H} and underestimate them by the same factor at $N_{\text{H}} = 10^{22} \text{ cm}^{-2}$. Finally we note that with a 10^7 K thin thermal energy distribution, the absorbed X-ray count rate to optical flux ratio remains constant within a factor of 2 for a large range of N_{H} and that therefore, the estimated X-ray to bolometric luminosity ratio is relatively unaffected by errors on the intervening column density.

Another problem arises from the unavoidable incompleteness of the data listed in SIMBAD. Several stars lack precise spectral types and/or magnitudes. Keeping in mind our concern to select the most obvious accreting candidates, in order not to overestimate the X-ray to bolometric luminosity ratio we used as default value B0 for all stars without subtypes and luminosity class III for all stars lacking appropriate information. When the B-V colour was not available we arbitrarily assumed B-V = 0.0. These default assumptions imply that we may have missed a fraction of the low $L_{\text{X}}/L_{\text{bol}}$ candidates. In the few cases when a range of spectral types and luminosity classes was available, we used the average value. For early type stars, the difference in intrinsic colours and bolometric corrections between two consecutive spectral types or luminosity classes is always small compared to other uncertainties.

We show in Fig. 1 the distribution of all X-ray/OB star identifications having spectral types earlier than or equal to B5 and located within r_{95} , the 95% confidence radius of the ROSAT position, in the $L_{\text{X}}/L_{\text{bol}}$ versus HR2 diagram. The hardness ratio HR2 is more sensitive to the intrinsic shape of the spectrum while the softer HR1 is rather an indicator of the photoelectric absorption. Most OB stars cluster at $L_{\text{X}}/L_{\text{bol}}$ between 10^{-7} and 10^{-6} as expected from previous studies carried out with the Einstein satellite (Pallavicini et al. 1981, Sciortino et al. 1990). Simulations show that indeed the slight variation in energy range from Einstein (0.2-4.0 keV) to ROSAT (0.1-2.4 keV) does not significantly change the X-ray luminosities derived from the two satellites. Similar values of $L_{\text{X}}/L_{\text{bol}}$ were also derived from a subsample of ROSAT survey data (Meurs et al. 1992). We did not investigate possible differences between OB and OBe stars in our sample. Most normal OB stars have HR2 values comprised between -0.7 and +0.3 which correspond to thin thermal temperatures in the range of $3 \cdot 10^6 \text{ K}$ to $3 \cdot 10^7 \text{ K}$ in agreement with those usually reported for normal OB stars. In contrast, the known massive X-ray binaries detected in the galactic plane exhibit larger luminosity ratios and a much harder HR2 which probably reflects the intrinsically harder power law-like energy distribution of accreting neutron stars and also maybe to a lower extent the often large interstellar and intrinsic column densities. We note, however, that luminous soft X-ray components were detected in some massive X-ray binaries accreting from the wind of the primary (e.g. 4U 1700-37; Haberl et al. 1994)

or through Roche lobe overflow (e.g. LMC X-4; Dennerl 1991). This last source is located in a direction of low interstellar absorption and exhibits $\text{HR1} = 0.36 \pm 0.01$; $\text{HR2} = -0.20 \pm 0.01$. Because of the sometimes large orbital phase dependent circumstellar absorption, the presence of a soft X-ray excess, although clearly detectable from the relative strength of the hard (2-10 keV) and soft (0.1-2 keV) un-absorbed components, does not necessarily imply a very soft value of HR1 or HR2 in the ROSAT band (e.g. 4U 1700-37; Haberl et al. 1994). On the other hand, Be/X-ray systems seem to lack a soft component (Haberl 1994).

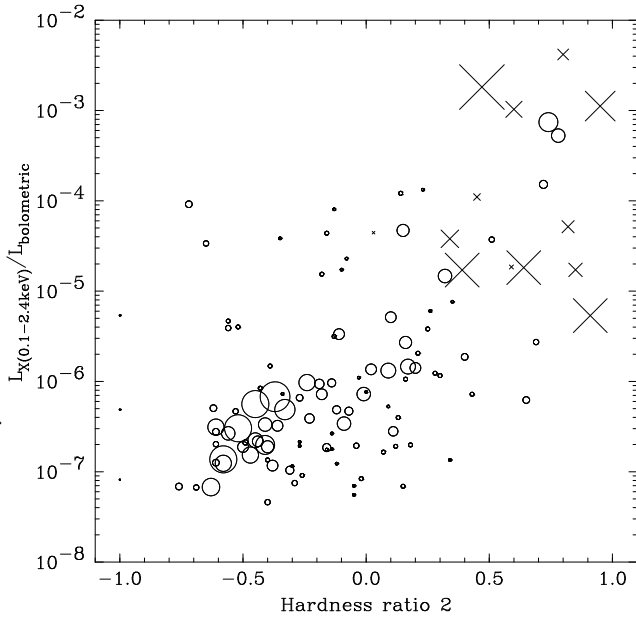


Fig. 1. Distribution of all X-ray/OB star identifications having spectral types earlier or equal to B5 and located within the 95% confidence radius in the $L_{\text{X}}/L_{\text{bol}}$ versus HR2 diagram. Open circles represent the ROSAT OB identifications and crosses represent the known high mass X-ray binaries detected during the ROSAT all-sky survey and located at absolute galactic latitudes below 20° . The size of the symbols is inversely proportional to the error on HR2. While most ROSAT OB star identifications cluster in the narrow range of $L_{\text{X}}/L_{\text{bol}}$ ratio similar to that derived from Einstein observations, all established X-ray binaries appear with clear X-ray excess and much harder X-ray spectra than normal OB stars

By contrast, it can be seen on Fig. 2 that B6 to B9 stars exhibit a much larger $L_{\text{X}}/L_{\text{bol}}$ ratio than earlier types and also a somewhat larger scatter. This behaviour was already noticed by Meurs et al. (1992). Obviously these late B stars do not obey the same relation as hotter types. The range of HR2, however, is comparable to that observed in earlier B stars. Einstein observations of nearby A type

stars by Schmitt et al. (1985) showed that none of these stars had any detectable X-ray emission. Nevertheless, the Einstein observatory detected several A type stars in the Pleiades cluster (Micela et al. 1990) and more recently several field A stars were detected in the ROSAT all-sky survey (Schmitt et al. 1993). These evidences led to the common assumption that the X-ray emission sometimes associated with late B or A stars was originating from an optically undetectable G-M type companion. However, ROSAT HRI observations seem to question this explanation and may point toward intrinsic X-ray emission at least in some late B stars (Berghöfer & Schmitt 1994). In spite of the high L_X/L_{bol} ratio the actual un-absorbed X-ray luminosities all remain below $2 \cdot 10^{32} \text{ erg s}^{-1}$ and only four stars exhibit X-ray luminosity in excess of $6 \cdot 10^{31} \text{ erg s}^{-1}$. Inspection of the optical maps of these four stars suggests the presence of likelier optical counterparts in the ROSAT error circle. Therefore, considering the absence of good candidates displaying X-ray luminosities above the level at which an interpretation in terms of an optically unseen late type companion star becomes untenable and the rather large expected number of spurious matches resulting from the size of the entry catalogue, we decided not to investigate the late B stars for the moment. Consequently, in the following, we shall only consider stars earlier than B6 or those having the general 'OB' type designation totaling 15895 stars.

2.5. Rate of spurious matches

We show in Fig. 3 the histogram of X-ray to optical distances for the 128 stars earlier than B6 associated with an X-ray source. The shape of the distribution shows without ambiguity that several OB stars were indeed detected during the ROSAT survey. The average 95% confidence radius for all OB star matches in the original cross-correlation list is $34''.5$. With a total of 15895 OB stars earlier than B6 and a mean survey source density of \approx one per square degree in the galactic plane (Motch et al. 1991b), roughly independent of galactic latitude and longitude (Voges 1992), we expect 5 spurious matches among the 108 spatial coincidences within r_{95} and 10 spurious matches among the 17 associations found in the range of 1 to $1.8 r_{95}$, this latter value corresponding to the $1'$ limit. The estimated number of real OB/X-ray associations within and outside r_{95} is 103 and 7 respectively, thus confirming the validity of the statistics used for the computation of error radii.

Because the number of non X-ray detected OB stars is much larger than the number of OB stars detected in the survey, we expect most spurious OB/RGPS source associations to be with non detected early type stars and therefore to be preferentially found in the high L_X/L_{bol} samples. Consequently, the recognition of a genuine accreting source requires additional information which may be the X-ray spectral or temporal behaviour and/or follow-up optical searches for alternative optical counterparts, essen-

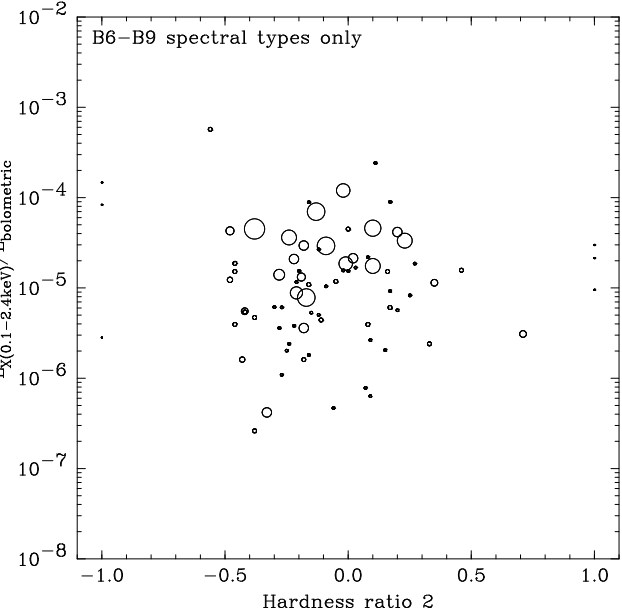


Fig. 2. Distribution of all X-ray/OB star identifications having spectral types B6 to B9 and located within the 95% confidence radius in the L_X/L_{bol} versus HR2 diagram. The size of the symbols is inversely proportional to the error on HR2. Late B stars do not follow the same L_X/L_{bol} relation as earlier spectral types (see Fig. 1) and exhibit a large scatter. At the count statistics typical of survey data, their hardness ratios HR2, however, are not essentially different from those of O-B5 stars

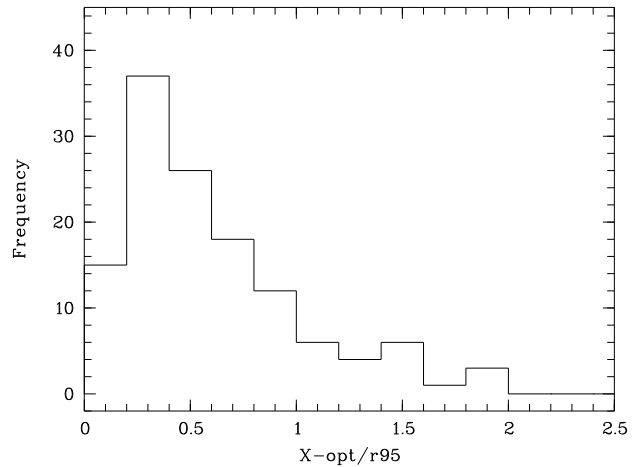


Fig. 3. Histogram of the distances between the SASS and SIMBAD positions for the 128 stars earlier than B6 associated with a ROSAT all-sky survey source. X-ray to optical distances are expressed in units of the 95% confidence error radius

tially active coronae in the galactic plane. For the B6-B9 stars, we expect ≈ 6 spurious spatial coincidences among the 79 located within the 95% confidence radius implying that these random associations cannot explain the systematically higher L_X/L_{bol} ratio exhibited by these late B stars.

2.6. Selection of the candidate stars

Using the computed luminosity ratio and optical / X-ray positional information we selected three different sets of candidate OB/X-ray binaries as defined in Table 4. The use of the 95% confidence radius was guided by the fact that the expected number of spurious matches within r_{95} (≈ 5) was about the same as the number of true associations expected to be located outside this radius. However, when referring to the accuracy of the X-ray positions we will mention the 90% confidence radius in order to be consistent with commonly used conventions in X-ray astronomy. The lower limit of $L_X/L_{bol} = 3 \times 10^{-6}$ is the maximum ratio observed for normal OB stars with the Einstein satellite (Sciortino et al. 1990). As a final criterion we removed 3 stars displaying X-ray luminosities below $10^{31} \text{ erg s}^{-1}$ since as already argued above, these luminosities may be radiated by the most active late type coronae. The 3 stars (HD 37272, HD 180939 and HD 68518) all have B5V spectral types and L_X/L_{bol} in the range $4-6 \times 10^{-6}$.

Table 4. Definition of the three groups of OB/X-ray binary candidates

Group	L_X/L_{bol}	dist(opt-X)
1	$\geq 10^{-5}$	$\leq r_{95}$
2	$\geq 10^{-5}$	$> r_{95}$
3	$3 \times 10^{-6}-10^{-5}$	$\leq r_{95}$

For comparison, all but one known massive X-ray binaries detected by ROSAT fall into candidate group 1. None appears in group 2 and the only one listed in group 3 is 4U 1700–37 / HD 153919 which consists of a neutron star accreting in the wind of a hot and luminous O6.5Iaf+ star (Walborn 1973; Haberl et al. 1994).

We then searched the literature in order to check for possible errors in the spectral type listed in each SIMBAD object header and more generally with the aim to find evidences for an alternative explanation to the observed X-ray emission such as a referenced late type companion or a white dwarf.

As a final check we analyzed interactively each remaining source with the dedicated Extended Scientific Analysis System (EXSAS) developed at MPE (Zimmermann et al. 1992). Whereas SASS operated on distinct survey strips, EXSAS has the capability to use all photons detected from a given region of the sky ($1^\circ \times 1^\circ$ merged fields in

our case) thus yielding improved background determination and source detection. For most sources, count rates, positions and hardness ratios derived from the interactive analysis were fully consistent with those given by the SASS output. We note that some of the positions computed by EXSAS were $10''$ or more away from the SASS determinations but still compatible within the errors. This slight change of X-ray position together with the use of refined optical coordinates extracted from the Guide Star Catalogue (GSC; Lasker et al. 1990) for 'LS' stars explains the difference between X-ray to optical distances listed in Table 5 and those appearing in individual finding charts and later Tables.

However, in a few instances, the EXSAS process derived count rates significantly lower than those given by SASS. In four cases (CPD –59 2854, LS III +58 47, HD 313343 and LS 4287), the SASS source was hardly or even not recovered at all by EXSAS and therefore dropped from the final list. These discrepancies could be related to the different data analyzed by the two processes. Survey spectra were accumulated for each source and light curves were systematically checked for variability and for the presence of features characteristic of a survey artifact.

The final list of SASS/SIMBAD OB/X-ray candidates containing 24 entries is printed in Table 5.

3. Follow-up observations

Each entry of the final SASS/SIMBAD list of candidate OB/X-ray binaries was then scheduled for follow-up optical observations. The main goals of the optical observations were to search for alternative identifications close to the X-ray position and to acquire better spectral classification of the OB candidate. Sources which had passed the optical investigation and which were not falling serendipitously in one of the ROSAT pointings were the scope of a dedicated AO-3 proposal.

3.1. Optical

For the southern hemisphere, optical observations were acquired mainly at ESO with the ESO-MPI 2.2 m + EFOSC2 (Buzzoni et al. 1984) during a run in 1992 from April 17 till 25. Low and medium resolution spectroscopy was obtained using respectively grism #6 ($\lambda\lambda 4500-7100 \text{ \AA}$; FWHM resolution $\approx 5.4 \text{ \AA}$), #3 ($\lambda\lambda 3500-5400 \text{ \AA}$; FWHM resolution $\approx 3.8 \text{ \AA}$), #7 ($\lambda\lambda 3550-4780 \text{ \AA}$; FWHM resolution $\approx 3.0 \text{ \AA}$) and #9 ($\lambda\lambda 5800-7000 \text{ \AA}$; FWHM resolution $\approx 3.0 \text{ \AA}$). In the imagery mode U, B, V and I frames were acquired with a pixel size of $0''.332$ and an exposure time of 2–5 min. In all cases, a THX #19 1024^2 CCD chip was used as detector. Spectra and images were corrected for bias and flat-field using standard MIDAS routines. Two-dimensional wavelength calibration was carried out using spectral lines of helium and argon lamps and the observation of standard stars allowed the flux calibration of a frac-

Table 5. The list of candidate OB/X-ray binaries scheduled for optical and X-ray follow-up observations. This table summarizes the preliminary values of spectral type, magnitude and star distance used as input of the automatic process in order to estimate L_X/L_{bol} and un-absorbed L_X . The input information was extracted from the SIMBAD header and results of the SASS analysis of the survey (see sections 2.1 & 2.4). When a range of spectral types and luminosity classes was available, we used the average value listed here. d_{O-X} is the distance between the SASS position and that of the associated OB star as read from the SIMBAD header. Errors listed here only arise from the PSPC count rate and do not take into account uncertainties on the detailed spectral type, interstellar absorption and distance. The horizontal lines divide the three groups of candidate stars defined in Table 4

Candidate Name	Spectral Type	B	d_{O-X} ('')	d (kpc)	L_X/L_{bol}	L_X (erg s^{-1})
LS I + 61 235	B5IIIe	12.15	7	1.3	$5.3 \pm 0.6 \ 10^{-4}$	$4.0 \pm 0.4 \ 10^{33}$
BSD 24- 491	B0e	11.39	35	4.1	$1.5 \pm 0.4 \ 10^{-5}$	$6.8 \pm 2.0 \ 10^{33}$
HD 38087	B5V	8.43	2	0.5	$4.7 \pm 0.8 \ 10^{-5}$	$6.9 \pm 0.7 \ 10^{31}$
HD 53339	B3V	9.44	28	1.1	$1.7 \pm 0.5 \ 10^{-5}$	$1.3 \pm 0.4 \ 10^{32}$
HD 59364	B5V	8.96	32	1.0	$9.2 \pm 2.9 \ 10^{-5}$	$1.3 \pm 0.4 \ 10^{32}$
HR 2875	B5Vp	5.27	29	0.2	$2.3 \pm 0.2 \ 10^{-5}$	$3.4 \pm 0.3 \ 10^{31}$
HD 67785	B2II	10.10	22	4.0	$4.4 \pm 1.0 \ 10^{-4}$	$4.9 \pm 1.1 \ 10^{33}$
LS 992	B	12.82	33	11.4	$7.4 \pm 0.7 \ 10^{-4}$	$3.3 \pm 0.3 \ 10^{35}$
LS 1698	B	12.20	22	18.2	$1.5 \pm 0.6 \ 10^{-4}$	$6.7 \pm 2.7 \ 10^{34}$
HD 165424	B4II	9.30	24	7.1	$3.8 \pm 1.7 \ 10^{-5}$	$3.1 \pm 1.4 \ 10^{33}$
LS 5039	B	12.17	6	3.2	$3.7 \pm 0.9 \ 10^{-5}$	$1.6 \pm 0.4 \ 10^{34}$
LS IV -12 70	B	12.00	57	16.6	$1.2 \pm 0.3 \ 10^{-4}$	$5.4 \pm 1.5 \ 10^{34}$
LS III +46 11	B	12.28	26	1.5	$1.5 \pm 0.2 \ 10^{-5}$	$6.5 \pm 0.8 \ 10^{33}$
BD +60 282	B1III	11.02	54	3.7	$1.6 \pm 0.7 \ 10^{-5}$	$1.6 \pm 0.7 \ 10^{33}$
LS I +61 298	B	11.40	54	12.6	$1.7 \pm 0.7 \ 10^{-5}$	$7.4 \pm 2.8 \ 10^{33}$
HD 38023	B4V	9.17	32	0.6	$1.8 \pm 0.6 \ 10^{-5}$	$4.2 \pm 1.4 \ 10^{31}$
LS V +29 14	B	11.20	41	11.5	$2.6 \pm 1.3 \ 10^{-5}$	$1.1 \pm 0.5 \ 10^{34}$
LS 3122	B	11.40	47	12.6	$8.8 \pm 2.4 \ 10^{-5}$	$3.9 \pm 1.1 \ 10^{34}$
SS 73 49	Be	13.50	57	2.1	$2.6 \pm 0.9 \ 10^{-5}$	$1.1 \pm 0.4 \ 10^{34}$
LS 5038	B	11.00	51	10.5	$2.9 \pm 1.1 \ 10^{-5}$	$1.3 \pm 0.5 \ 10^{34}$
LS IV -05 35	B	11.90	28	15.8	$8.6 \pm 2.4 \ 10^{-5}$	$3.8 \pm 1.1 \ 10^{34}$
HD 36262	B3V	7.52	17	0.6	$5.1 \pm 1.5 \ 10^{-6}$	$4.0 \pm 1.2 \ 10^{31}$
HD 161103	B2IVe	9.13	28	0.9	$7.6 \pm 4.1 \ 10^{-6}$	$1.8 \pm 1.0 \ 10^{32}$
SAO 49725	B0e	9.60	12	2.7	$3.8 \pm 1.1 \ 10^{-6}$	$1.7 \pm 0.6 \ 10^{33}$

tion of the spectra. Additional spectroscopy was obtained from 1994 February 10 till 14 with the ESO 1.5m telescope and the Boller & Chivens instrument. Finally some spectra were also obtained using the Cassegrain Boller & Chivens spectrograph attached at the 1.6m telescope of the Brazilian Laboratorio Nacional de Astrofisica (LNA; Brazopolis, Brazil). The detector used was a 770×1152 GEC CCD and the FWHM resolution was $\approx 9 \text{ \AA}$ in the range $\lambda\lambda 3800\text{-}8200 \text{ \AA}$.

Northern fields were investigated during several observing runs performed at the Observatoire de Haute-Provence, CNRS, France, between 1990 November and 1995 January. This observing programme was part of a general project aiming at the optical identification and follow-up observations of area and X-ray selected sources extracted from the ROSAT Galactic Plane Survey. All OHP spectroscopic observations were obtained with the CARELEC spectrograph (Lemaitre et al. 1990) attached at the 1.93m telescope. Low resolution spectroscopy ($\lambda\lambda 3500\text{-}7500 \text{ \AA}$; FWHM resolution $\approx 14 \text{ \AA}$) and blue and red medium resolution spectroscopy ($\lambda\lambda 3800\text{-}4300 \text{ \AA}$; FWHM resolution $\approx 1.8 \text{ \AA}$, $\lambda\lambda 6300\text{-}6700 \text{ \AA}$; FWHM resolution

$\approx 1.7 \text{ \AA}$) were acquired using a 260 \AA/mm grating and a 33 \AA/mm grating respectively. Spectra were calibrated in wavelength using arcs of iron, neon and helium lamps. Observations of standard stars allowed to formally calibrate in flux all spectra. However, bad meteorological conditions which prevailed in some cases and the narrow slit used for some bright stars may bias the mean flux level on occasions and therefore, the spectrophotometric flux scale should be considered with some caution. CCD images were collected using the standard camera at the 1.2m telescope. Most of the time the Johnson B,V, and I filters were used. Depending on the CCD mounted, the field of view was either $7.1' \times 4.4'$ (RCA) or $6.5' \times 6.5'$ (TK512).

Spectral types of OB stars were derived comparing with spectral atlases in Jaschek & Jaschek (1987) and Walborn & Fitzpatrick (1990) and equivalent widths listed in Didelon (1982). For the later spectral types we used the atlas by Turnshek et al. (1985). Interstellar absorption was usually estimated from the $\lambda 4430$ and $\lambda 6284$ interstellar bands corrected for atmospheric effects and following the relations given in Krelowski et al. (1987) and Bromage & Nandy (1973).

3.2. X-ray

We list in Tables 6 and 7 the main X-ray characteristics of the sources derived both from survey and pointed PSPC data. Sources appear in each group ordered by increasing right ascension. All pointed X-ray data presented below were analyzed using the EXSAS package. Spectra were accumulated for each source and the light curves were checked for variability. We systematically searched all major catalogues produced by past X-ray instrumentation for a possible previous detection of the ROSAT source.

4. Criteria for the identification of OB/X-ray candidates

The goal of the present work is merely to extract from the ROSAT Galactic Plane Survey the most obvious OB/X-ray candidates. As stated in section 2.2, we decided to ignore for the moment all associations of a survey source with groups of OB stars and all cases where there was a possible alternative candidate to the OB identification. We applied the same strategy during the follow-up observations, dropping the candidate as soon as another possible optical counterpart was found.

Active coronae constitute up to 85% of the ROSAT survey sources at $b = 0^\circ$ (Motch et al. 1996b) and over 50% in the overall RGPS region (Motch et al. 1991b). Although no direct conspicuous signature of coronal activity exists in the optical spectra of late type stars, it is known that chromospheric and coronal activities tightly correlate in the Sun and F-M stars in general. In particular, Einstein observations have shown that the luminosity of the chromospheric Balmer and Ca II H&K emission lines is well correlated with the soft X-ray luminosity in Me stars (e.g. Fleming et al. 1988) and in F-G stars (e.g. Maggio et al. 1987). Using medium resolution blue optical spectra of ≈ 100 late type stars identified with RGPS sources with measured Ca II re-emission, Guillout (1996) find a very good correlation between Ca II H&K and soft X-ray emission with $L_{\text{CaII}} \sim L_{\text{X}(0.1-2.4\text{keV})}^{1.05 \pm 0.20}$. Because the slope in luminosity is close to 1, there also exists a useful relation between chromospheric fluxes and PSPC count rates r ; $F_{\text{CaII}} \sim r^{0.74 \pm 0.14}$ with a 0.1 PSPC cts s^{-1} corresponding to $F_{\text{CaII(H+K)}} \approx 2 \cdot 10^{-13} \text{ erg cm}^{-2} \text{ s}^{-1}$. These relations hold over 2 decades in flux and over 3 decades in luminosity. A rms scatter of about a factor 2 is present in flux and luminosity around the mean relation with a maximum deviation of a factor 10 above or below. The intrinsic long (solar cycles) and short (flares) time scales of variability and the non-simultaneity of the optical follow-up / X-ray survey observations probably account for the rather large scatter. We checked that the measured chromospheric fluxes and PSPC count rates of all late type stars proposed as alternative identification to the early type star were compatible with the relation of Guillout (1996). Because of the sometimes inaccurate spectrophotometry we re-calibrated our blue medium resolution spectra using either magnitudes extracted from the literature or derived from our CCD images.

In the absence of alternative candidates, we used the X-ray luminosity as additional criterion. Although active coronae with X-ray luminosities above $10^{31} \text{ erg s}^{-1}$ are usually not observed in late type stars (see e.g. Rosner et al. 1985) some RS CVns (Ottmann & Schmitt 1992) and extreme T Tauri stars (e.g. Montmerle et al. 1983) do exhibit on occasions soft X-ray luminosities above $10^{31} \text{ erg s}^{-1}$. Accordingly, candidate stars with excess L_{X} in the range of $10^{31-32} \text{ erg s}^{-1}$ were indicated as deserving further attention but are not considered as very good candidates.

The last criterion considered is the hardness of the source. Normal OB stars usually exhibit $\text{HR2s} \leq 0.3$ whereas most HMXBs known prior to the launch of ROSAT have hard $\text{HR2s} \geq 0.4$. However, the separation power of this X-ray spectral criterion is decreased by the presence of a soft excess in a small fraction of these OB/X-ray systems (e.g. LMC X-4). Furthermore, some very active coronae may also display hard spectra (e.g. Schmitt et al. 1990) and a fraction of T Tauri stars exhibit hardness ratios HR2 larger than 0.4 (e.g. Neuhauser et al. 1995). We did not consider the presence or absence of Balmer emission lines as a criterion since some early type companions of known massive sources lack these spectral features.

Finally, in spite of the large galactic absorption expected in the directions occupied by OB stars, a few bright extragalactic emitters may still shine in X-ray through the galactic fog. These sources will also display a hard HR2 as a result of interstellar absorption and will be optically faint ($V \lesssim 18$). The detection of characteristic features in their optical spectra may be beyond the capability of the instrumentation used for this project. Motch et al. (1996b) estimate that the spatial density of extragalactic emitters in the RGPS Cygnus test region is $2.7 \cdot 10^{-2}$ extragalactic sources per square degree brighter than 0.02 ct s^{-1} for b in the range of -5° to $+5^\circ$. If these densities are typical of the average OB star directions, we expect ≈ 0.1 spurious coincidence within a typical 95% confidence radius between an extragalactic emitter and an OB star. Therefore, we cannot completely rule out the possibility that at least one of the investigated candidate sources is actually extragalactic.

5. Results from individual source observations

5.1. Accreting candidates

5.1.1. VES 625 = LS I +61 235 (Group 1)

This Be/X-ray system was discovered by Motch et al. (1991b) as a result of a preliminary investigation of the ROSAT Galactic Plane Survey. It actually stands out from Table 5 as exhibiting one of the largest $L_{\text{X}}/L_{\text{bol}}$. Optical observations revealed only moderate Balmer emis-

Table 6. Positions and errors resulting from the EXSAS analysis of survey and pointed PSPC observations of the OB/X-ray candidates selected for follow-up observations. We also list the difference between the X-ray pointed and optical positions (p-o) and difference between pointed and survey positions (p-s). The optical positions used here are the most accurate available for each OB target and not necessarily those used in Table 4. Column (o.a.) lists the off axis angle for the pointed observations. Source names are computed after the survey EXSAS positions. Horizontal lines divide the three groups of candidates defined in Table 4

Candidate Name	ROSAT Source Name	Source position (2000.0)										o.a.	Pointing Identification
		p-o (")	p-s (")	Survey		r ₉₀ (")	Pointed observations			r ₉₀ (")			
				α (h m s)	δ (° ' '')	α (h m s)	δ (° ' '')	α (h m s)	δ (° ' '')	α (h m s)	δ (° ' '')		
LS I +61 235	RX J0146.9+6121	5	9	01 46 59.5	+61 21 22	24	01 47 00.8	+61 21 22	17	24	UK 400332		
BSD 24- 491	RX J0440.9+4431	6	38	04 40 57.5	+44 31 22	36	04 40 59.9	+44 31 51	17	0.8	WG 400397		
HD 38087	RX J0542.9-0218	18	19	05 42 59.8	-02 18 46	23	05 43 00.2	-02 18 28	19	35	WG 900189/386		
HD 53339	RX J0704.2-1123			07 04 14.1	-11 23 47	50							
HD 59364	RX J0728.6-2629			07 28 38.2	-26 29 12	43							
HR 2875	RX J0729.0-3848			07 29 05.2	-38 48 15	20							
HD 67785	RX J0807.2-5053			08 07 12.8	-50 53 12	22							
LS 992	RX J0812.4-3114			08 12 28.4	-31 14 51	21				30	WG 400315		
LS 1698	RX J1037.5-5647	3	16	10 37 33.7	-56 47 49	25	10 37 35.2	-56 47 59	21	0.2	WG 400394		
HD 165424	RX J1806.8-2606	40	55	18 06 53.9	-26 06 25	33	18 06 57.5	-26 06 00	17	1.2	WG 400396		
LS 5039	RX J1826.2-1450	13	13	18 26 14.9	-14 50 29	22	18 26 14.8	-14 50 42	35	41	US 400285		
LS IV -12 70	RX J1830.7-1232	96	73	18 30 45.8	-12 32 28	67	18 30 50.8	-12 32 29	24	31	WG 500040		
LS III +46 11	RX J2035.2+4651	6	1	20 35 12.9	+46 51 16	19	20 35 13.0	+46 51 17	18	0.4	WG 400393		
BD +60 282	RX J0136.7+6125			01 36 43.2	+61 25 59	29							
LS I +61 298	RX J0234.4+6147	19	40	02 34 29.1	+61 47 49	56	02 34 34.0	+61 47 29	30	24	WG 201263		
HD 38023	RX J0542.3-0807	18	22	05 42 19.1	-08 07 45	26	05 42 20.0	-08 08 02	18	16	US 200901		
LS V +29 14	RX J0553.0+2939			05 53 02.2	+29 39 11	24							
LS 3122	RX J1335.5-6211			13 35 33.6	-62 11 04	22							
SS 73 49	RX J1559.2-4157			15 59 14.2	-41 57 57	44							
LS 5038	RX J1826.1-1321	93	59	18 26 11.7	-13 21 57	35	18 26 14.1	-13 21 09	25	14	US 400283		
LS IV -05 35	RX J1900.7-0503			19 00 45.7	-05 03 50	22							
HD 36262	RX J0531.0+1206			05 31 02.3	+12 06 03	23							
HD 161103	RX J1744.7-2713	5	21	17 44 44.5	-27 13 30	28	17 44 45.4	-27 13 47	18	0.6	WG 400400		
SAO 49725	RX J2030.5+4751	5	13	20 30 31.1	+47 51 58	35	20 30 30.6	+47 51 46	18	0.4	WG 400393		

sion (EW (H α) = -7, -10 Å) with a distinct absorption core on occasions (Coe et al. 1993). Follow-up ROSAT pointed PSPC observations by Hellier (1994) showed that the source was pulsating with a 1412 s period thus being the slowest Be/neutron star known. Together with the nearby unusual ultrasoft 8.7 s pulsar (Israel et al. 1994), RX J0146.9+6121 = LS I +61 235 contributes to the Uhuru source 4U 0142+61. The energy distribution of RX J0146.9+6121 is hard with a power law energy index of -0.6 ± 0.7 (Hellier 1994) in agreement with the very positive HR1 and HR2 measured during the ROSAT all-sky survey.

Medium resolution blue spectroscopy obtained at OHP on 1992 October 23 and 1995 January 30 (see Fig. 4) indicates a spectral type significantly earlier than the B5III type proposed by Slettebak (1985). The relative strength of the Si III λ 4552 / He I λ 4387 suggests a giant luminosity class. For this class, the C III + O II blend at λ 4650 rather indicates an early B1 type. Therefore, although our spectral range may not be ideal for spectral classification, we believe that the star is hotter than previously thought and may be classified as a B1IIIe type star. The revised distance of LS I +61 235 ($d \approx 2.9$ kpc) is more consistent

with the distance of the open cluster in which it is located ($d = 2.5$ kpc; Tapia et al. 1991) than that derived from a B5III type ($d \approx 1.3$ kpc).

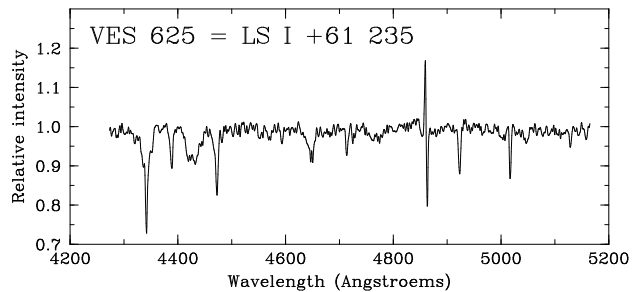


Fig. 4. Rectified blue medium resolution spectrum of VES 625 = LS I +61 235 obtained with the OHP 1.93 m and CARELEC spectrograph on 1995 January 30. Exposure time was 10 min

The Balmer emission lines exhibit dramatic V/R changes on time scales of two years or less as shown for the

Table 7. X-ray count rates and hardness ratios derived from survey and pointed observations for the 24 sources tentatively associated with OB/X-ray candidates and selected for follow-up observations. All data listed here were obtained using EXSAS with the exception of survey hardness ratios which are those listed in the SASS automatic analysis. For pointed observations, the maximum likelihood (ML) values are the largest of the broad (b) and hard (h) energy bands. For HD38087 count rates and exposure times are the mean and sum of pointings WG 900189 and WG 900386 whereas the ML and HRs correspond to WG900189 only. The horizontal lines divide the three groups of candidates defined in Table 4

Candidate Name	Survey					Pointed observations				
	count rate (10^{-3}s^{-1})	ML	exp (s)	HR1	HR2	count rate (10^{-3}s^{-1})	ML	exp (s)	HR 1	HR2
LS I +61 235	146 \pm 18	119	539	+0.89 \pm 0.10	+0.78 \pm 0.14	259 \pm 18	4531(b)	10749	+0.99 \pm 0.01	+0.70 \pm 0.02
BSD 24- 491	27 \pm 9	13	492	+0.75 \pm 0.22	-0.18 \pm 0.52	68 \pm 6	652(h)	2048	+0.95 \pm 0.05	+0.55 \pm 0.07
HD 38087	74 \pm 13	73	504	+0.82 \pm 0.17	+0.15 \pm 0.16	66 \pm 7	446(b)	47009	+1.00 \pm 0.06	+0.09 \pm 0.04
HD 53339	23 \pm 9	8	474	+0.77 \pm 0.20	-0.10 \pm 0.70					
HD 59364	35 \pm 11	11	431	-0.15 \pm 0.69	-0.72 \pm 0.34					
HR 2875	663 \pm 51	402	277	-0.98 \pm 0.02	-0.08 \pm 0.70					
HD 67785	45 \pm 9	40	763	+0.13 \pm 0.52	-0.16 \pm 0.53					
LS 992	285 \pm 27	311	449	+0.98 \pm 0.02	+0.74 \pm 0.09	\leq 3		19520	—	—
LS 1698	66 \pm 20	24	207	+0.74 \pm 0.23	+0.72 \pm 0.25	3.3 \pm 1.7	9.1(h)	1198	—	—
HD 165424	33 \pm 15	7	265	+0.76 \pm 0.30	-0.35 \pm 0.62	41 \pm 5	251(b)	2016	+1.00 \pm 0.05	+0.16 \pm 0.12
LS 5039	52 \pm 15	27	331	+0.92 \pm 0.08	+0.51 \pm 0.38	43 \pm 6	57(h)	7714	+0.86 \pm 0.29	+0.78 \pm 0.22
LS IV -12 70	17 \pm 10	4	342	+0.60 \pm 0.33	+0.14 \pm 0.52	36 \pm 2.5	98(h)	11896	+1.00 \pm 0.11	+0.31 \pm 0.08
LS III +46 11	59 \pm 10	60	872	—	+0.32 \pm 0.14	46 \pm 6	196(h)	1257	+1.00 \pm 0.05	+0.46 \pm 0.12
BD +60 282	17 \pm 7	12	540	—	-0.10 \pm 0.70					
LS I +61 298	11 \pm 5	7	631	+0.41 \pm 0.45	+0.16 \pm 0.69	13 \pm 2	33(h)	8841	—	+0.30 \pm 0.18
HD 38023	27 \pm 9	18	474	+0.54 \pm 0.38	-0.34 \pm 0.46	14 \pm 1	230(b)	15048	+0.95 \pm 0.05	-0.11 \pm 0.07
LS V +29 14	26 \pm 9	18	435	+0.29 \pm 0.49	-0.14 \pm 0.52					
LS 3122	64 \pm 19	23	265	+0.60 \pm 0.33	-0.26 \pm 0.51					
SS 73 49	46 \pm 20	8	177	+0.54 \pm 0.38	+0.01 \pm 0.71					
LS 5038	17 \pm 9	7	323	+0.69 \pm 0.37	+0.50 \pm 0.53	1.8 \pm 0.5	12(h)	8747	—	—
LS IV -05 35	41 \pm 12	24	373	+0.32 \pm 0.48	—					
HD 36262	49 \pm 12	36	467	+0.69 \pm 0.37	+0.26 \pm 0.66					
HD 161103	31 \pm 13	9	313	+0.28 \pm 0.65	+0.35 \pm 0.62	12.7 \pm 2.6	65(h)	2000	+0.94 \pm 0.17	+0.47 \pm 0.21
SAO 49725	8 \pm 4	7	920	+0.82 \pm 0.23	+0.25 \pm 0.50	19.5 \pm 4.2	62(h)	1286	+0.91 \pm 0.21	+0.35 \pm 0.23

$H\beta$ line in Fig. 5. Our red $H\alpha$ spectrum obtained on 1992 December 15 (see Fig. 6) is mirror-symmetric of that plotted in Coe et al (1993) and obtained on 1991 August 28, in the sense that the ‘violet’ component is much stronger than the ‘red’ one. The maximum time for the $H\alpha$ V/R reversal is of the order of 1.5 yr.

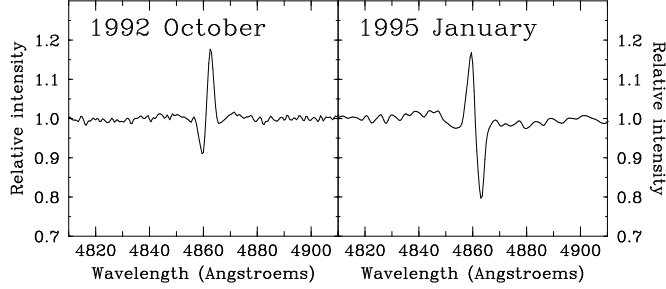


Fig. 5. Rectified blue medium resolution spectrum of VES 625 = LS I +61 235 obtained with the OHP 1.93 m and CARELEC spectrograph on 1992 October 23 and 1995 January 30 showing the large V/R changes having occurred in the 2 years interval

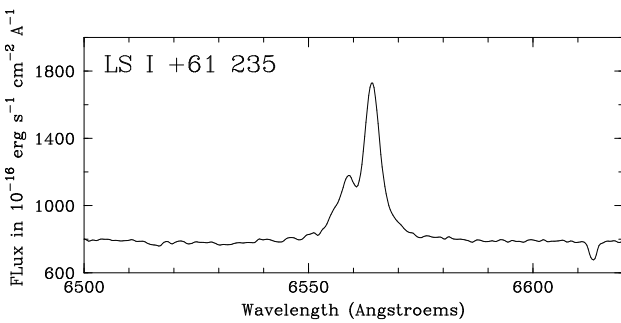


Fig. 6. Red medium resolution spectrum of VES 625 = LS I +61 235 obtained with the OHP 1.93 m and CARELEC spectrograph on 1992 December 15. Exposure time was 30 min

5.1.2. BSD 24- 491 (Group 1)

Visual inspection of the POSS O and E plates and B and I band CCD images failed to reveal any plausible alternative active corona counterpart within the error circles of the ROSAT survey and pointing positions. The star BSD 24-

491 = LS V +44 17 = VES 826 is referenced as a B0 star with indication for H α emission (Seyfert & Popper 1941; Coyne & McConnell 1983). Low resolution spectrum obtained on 1991 November 16 (see Fig. 7) shows clear evidence for H α emission with an EW = -2.0 ± 0.2 Å.

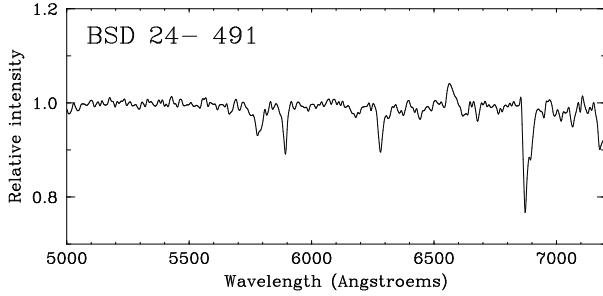


Fig. 7. Low resolution spectrum of BSD 24- 491 obtained on 1991 November 16 UT at OHP. The FWHM resolution is 15 Å. Relatively weak H α emission is clearly detected

A blue high resolution spectrum obtained on 1991 November 27 confirms the B0 type listed in SIMBAD for this star (see Fig. 8). There are no good luminosity sensitive lines in our wavelength range. However, the EW of He I λ 4471 rather suggests a dwarf or giant star (Dideion 1982). The photometry reported by Bigay (1963); V = 10.78, B-V = 0.61, U-B = -0.36 indicates a rather high interstellar absorption E(B-V) = 0.90 in agreement with the depth of the λ 4430 and λ 6284 interstellar bands. An additional medium resolution spectrum obtained at OHP in 1995 January reveals an increase of the Balmer emission compared to our observation in 1991 with strong double peaked H β and iron/He I lines in emission.

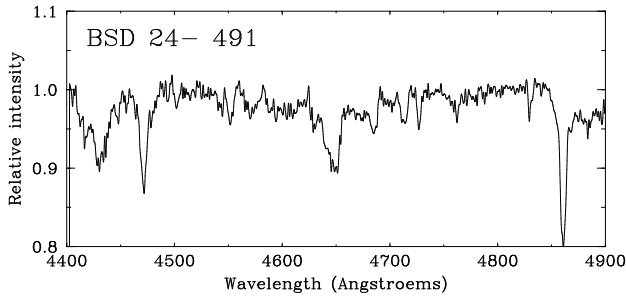


Fig. 8. Rectified blue medium resolution spectrum of BSD 24- 491 obtained on 1991 November 27 at OHP

The source was detected again during a dedicated pointed PSPC observation with a count rate ≈ 2.5 times higher than during survey observations. Our pointed observation indicates that the source is hard (HR2 = 0.55

± 0.07) and maybe variable (see Fig. 9). The position of the X-ray source derived from the pointed observation is only 6'' away from the GSC position of the Be star. From all these evidences we conclude that BSD 24- 491 is very likely to be a new Be/X-ray system.

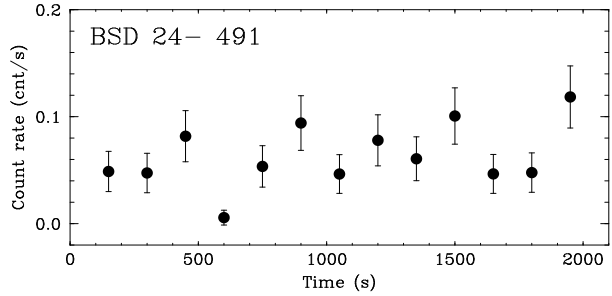


Fig. 9. The pointed observation 0.5-2.0 keV X-ray light curve of BSD 24- 491. Integration time is 150 s

5.1.3. LS 992 (Group 1)

LS 992 is one of the X-ray brightest and hardest new Be/X-ray candidates in the ROSAT all-sky survey. Close inspection of B and I images (see Fig. 10) failed to reveal any alternative optical counterpart to the X-ray source. Optical spectroscopy of object B, the second brightest in the error circle, suggests a late type star with H α and H β in absorption, leaving the B star as the most likely optical counterpart of RX J0812.4-3114. Our blue medium resolution spectrum of LS 992 is unfortunately somewhat too noisy to derive a very accurate spectral type. However, the Si III/IV and He I lines indicate a B0-1 spectral type and a luminosity class V to III (see Fig. 11). The red spectra show the presence of H α emission with a central absorption core (see Fig. 12) similar to that observed from LS 1698 (see below). The total H α equivalent width does not vary much over the one week interval between the two spectroscopic observations (EW(H α) = -4.6 ± 0.1 ; -4.9 ± 0.1 on 1992 April 18 and 25 respectively). However, the V/R ratio may have slightly evolved.

Optical photoelectric photometry by Reed (1990) gives V = 12.42; B-V = 0.41 and U-B = -0.69 in agreement with the B0-1 V-IIIe spectral type proposed. Assuming (B-V)₀ = -0.28 yields E(B-V) = 0.69, consistent with that derived from the depth of the λ 4430 and λ 6284 interstellar bands which imply E(B-V) = 0.7-1.0 and E(B-V) = 0.8 ± 0.2 respectively.

Although LS 992 is the second brightest X-ray binary candidate from the survey data, the statistics are still not good enough to really constrain the shape of the X-ray energy distribution. The spectrum is undoubtedly much harder (HR2 = $+0.74 \pm 0.09$) than normal OB star emission. Fitting simple power law models and fixing the col-

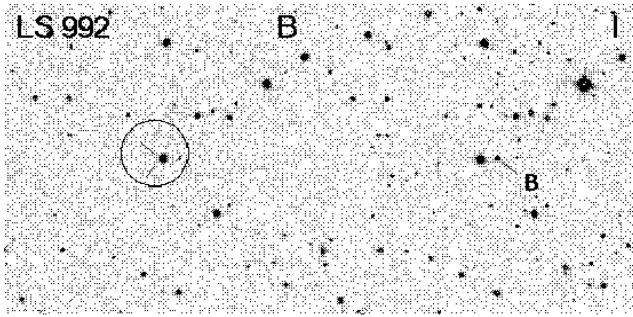


Fig. 10. B and I CCD images of the field of LS 992 obtained on 1992 April 18 with EFOSC2 and the ESO-MPI 2.2 m telescope. Both images have 2 min exposure time. North is at top and East to the left. Each frame is $2'83 \times 2'83$ wide. On the B image we plot the ROSAT survey 90% confidence error circle and show the position of LS 992. On the I band image we show the position of the alternative optical candidate “B” investigated spectroscopically and apparently unrelated to the X-ray source

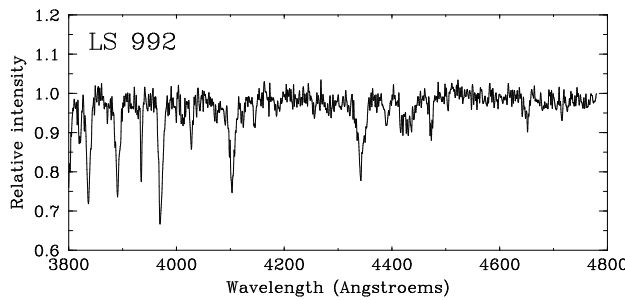


Fig. 11. Rectified blue medium resolution spectrum of LS 992 obtained with the ESO-MPI 2.2 m + EFOSC2 on 1992 April 18. Exposure time was 15 min

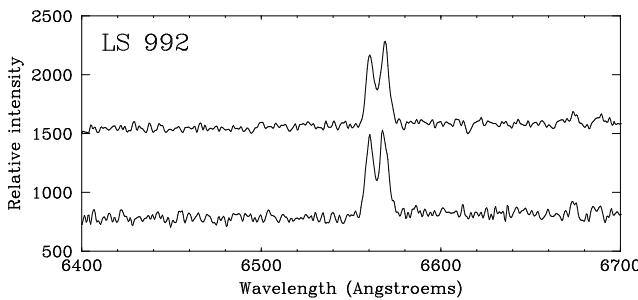


Fig. 12. Red medium resolution spectrum of LS 992 showing the H α emission. The upper spectrum was exposed 20 min on 1992 April 18 and the lower one 5 min on April 25. Both spectra were obtained with the ESO-MPI 2.2 m telescope

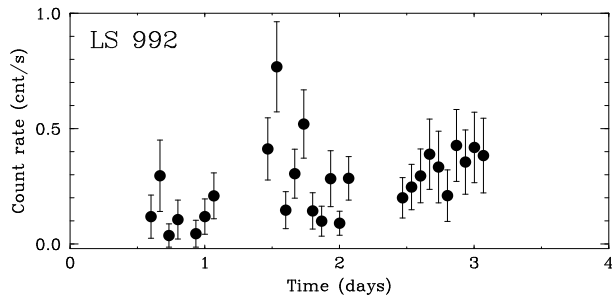


Fig. 13. Survey light curve of RX J0812.4–3114, the source associated with LS 992. Each data point corresponds to one satellite scan (10 to 32 s every 96 min) integrated between 0.4 and 2.4 keV. Time 0 is JD 2448192.5759

umn density at its interstellar value ($N_{\mathrm{H}} = 5 \cdot 10^{21} \mathrm{cm}^{-2}$) implies a photon index in the range of +0.5 to –1.5 (95% confidence level), well within the range observed from accreting neutron stars in massive X-ray binaries (White et al. 1983). The hard X-ray light curve plotted on Fig. 13 shows some evidence for variability.

A long follow-up pointed PSPC observation on 1992 November 20 failed to recover the source. A 3σ upper limit of $\approx 3 \cdot 10^{-3} \mathrm{ctss}^{-1}$ can be set to the count rate of RX J0812.4–3114, i.e. about 100 times fainter than during survey observations. Contemporaneous optical spectroscopy obtained at LNA, Brazil, on November 28 shows H α emission with an EW = -4.6 \AA , similar to that observed 7 months before at La Silla.

No catalogued X-ray source is found at the position of LS 992. The large long term flux variability, similar to that exhibited by many Be/X-ray transients and the X-ray hardness strongly suggest that LS 992 is a new accreting Be/X-ray system.

5.1.4. LS 1698 (Group 1)

Comparison of the I and B band CCD images failed to reveal any other bright or very red star in the error circle which could be an alternative active corona identification (see Fig. 14). In the red, H α is clearly seen in emission with a strong absorption core (see Fig. 15). The same H α profile was again observed in February 1994. Our medium resolution blue spectrum shown in Fig. 16 indicates a B0 V–IIIe type star. The strength of the $\lambda 4430$ and $\lambda 6284$ interstellar bands suggests a rather large interstellar absorption $E(B-V) = 0.75 \pm 0.25$. Using the GSC V magnitude and taking into account the reddening estimated from interstellar bands lowers the distance of LS 1698 from 18 kpc to ≈ 5 kpc.

The source was again detected during a dedicated pointed observation with a count rate about 20 times lower. The survey energy distribution characterized by HR2 is hard and HR1 is consistent with the large inter-

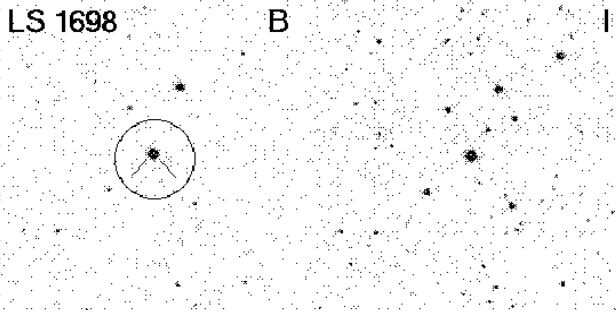


Fig. 14. B and I CCD images of the field of LS 1698 obtained on 1992 April 17 with EFOSC2 and the ESO-MPI 2.2 m telescope. Both images have 2 min exposure time. North is at top and East to the left. Each frame is 2.83×2.83 wide. On the B image we plot the ROSAT pointing 90% confidence error circle and show the position of LS 1698

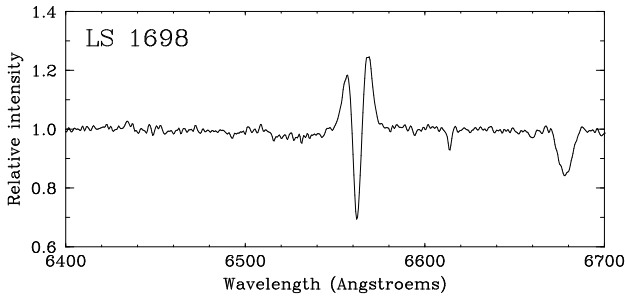


Fig. 15. Rectified red medium resolution spectrum of LS 1698 showing the $\text{H}\alpha$ emission. This spectrum (15 min exposure time) is the sum of two spectra obtained on 1992 April 15 and 17 with the ESO-MPI 2.2 m telescope

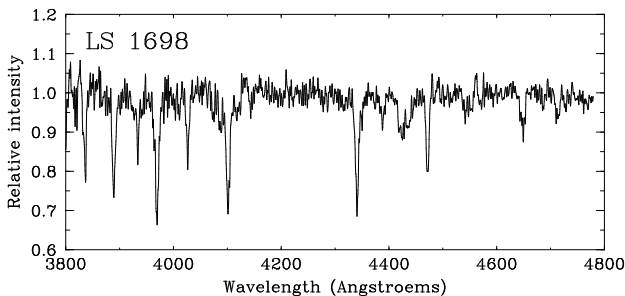


Fig. 16. Rectified blue medium resolution spectrum of LS 1698 obtained with the ESO-MPI 2.2 m + EFOSC2 on 1992 April 17. Exposure time was 10 min

stellar absorption. From these evidences, we conclude that LS 1698 is most probably a new Be/X-ray system.

We note that LS 1698 is the likely optical counterpart of the hard X-ray transient source 4U1036–56/3A 1036–565. Its position lies well inside the error box of the Uhuru source and close to the Ariel V position and the ROSAT survey source is the only one in the Uhuru and Ariel error boxes. The former identification of 3A 1036–565 with the bright Be star HD 91188 (Buckley et al. 1985) is thus probably not valid since the star lies quite outside the error box and is furthermore not detected in the ROSAT all-sky survey.

The source was first observed by the Uhuru satellite (Forman et al. 1978) and OSO 7 (Markert et al. 1979). Ariel V observed a flare in November 1974 (Warwick et al. 1981). At maximum flare the flux was $\approx 2.4 \cdot 10^{-10} \text{ erg cm}^{-2} \text{ s}^{-1}$ (2-10 keV) while the mean Uhuru flux was $\approx 1.0 \cdot 10^{-10} \text{ erg cm}^{-2} \text{ s}^{-1}$ (2-10 keV). During the survey, ROSAT detected a flux about 10 times less than during the years 1970-1976.

5.1.5. LS 5039 (Group 1)

From our B and I band images of the field of LS 5039 we could select 3 alternative candidate stars designated B,C and D on Fig. 17. Low resolution spectroscopic observations of these stars failed to reveal spectral signatures of any known class of galactic or extragalactic X-ray sources. All three candidates exhibit $\text{H}\alpha$ in absorption. Object B is an early M star. However, it lacks the Balmer emission which is nearly always found in X-ray active M stars (see e.g. Fleming et al. 1988; Motch et al. 1996b). Object C and D are too faint to be easily classified. Therefore, LS 5039 constitutes the most likely optical counterpart of the X-ray source.

The medium resolution blue spectrum of LS 5039 shown on Fig. 18 is typical of an O7V star with well marked $\text{He II } \lambda 4686$ absorption and some evidence for weak $\text{N III } \lambda 4634\text{--}4642$ emission, i.e. an O7V((f)) classification. No $\text{H}\alpha$ emission is present in our medium resolution red spectrum.

The optical photometry reported by Drilling (1975) gives $V = 11.23$, $B-V = 0.94$, $U-B = -0.16$. A $(B-V)_0 = -0.32$ implies $E(B-V) = 1.26$, a value slightly larger than that derived from the $\lambda 4430$ and $\lambda 6284$ interstellar band which both point at $E(B-V) = 0.8 \pm 0.2$.

During survey observations the X-ray source was one of the hardest of the OB/X-ray correlation list. The source was detected again during a subsequent PSPC pointing. The X-ray position derived from this observation is completely consistent with the survey position. The count rate is close to that of the survey but owing to the longer exposure time the slightly improved statistics allows to confirm the hardness of the source, clearly compatible with an accreting neutron star or black hole seen through the large intervening column density.

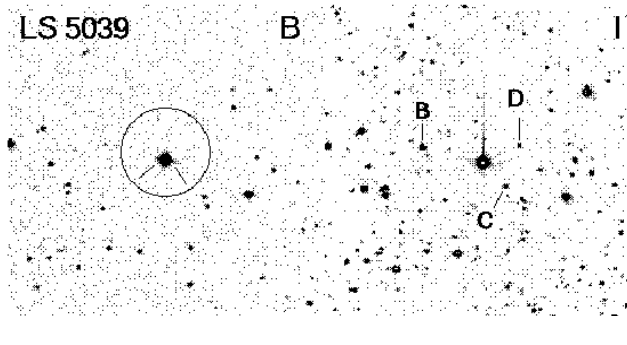


Fig. 17. B and I CCD images of the field of LS 5039 obtained on 1992 April 19 with EFOSC2 and the ESO-MPI 2.2 m telescope. Both images have 2 min exposure time. North is at top and East to the left. Each frame is 2.83×2.83 wide. On the B image we plot the ROSAT survey 90% confidence error circle and show the position of LS 5039. On the I band image we show the position of the alternative optical candidates investigated spectroscopically and apparently unrelated to the X-ray source

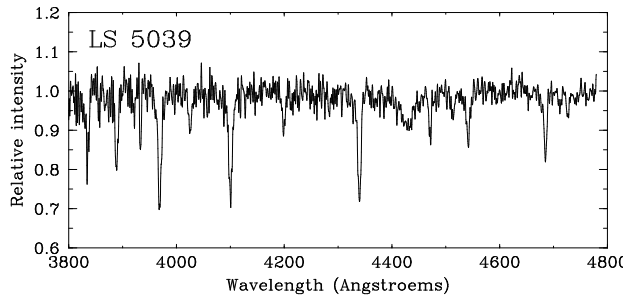


Fig. 18. Rectified blue medium resolution spectrum of LS 5039 obtained with the ESO-MPI 2.2 m + EFOSC2 on 1992 April 19. Exposure time was 5 min

In spite of the slight increase of the bolometric correction with respect to the automatic process which assumed a B0 III type, the updated L_X/L_{bol} ratio remains high (10^{-5}), exceeding by an order of magnitude at least that expected from normal O stars. We conclude that LS 5039 is a likely massive X-ray binary in which the compact object may accrete from the O star high velocity wind.

5.1.6. HD 161103 (Group 3)

HD 161103 is a relatively bright and variable ($V = 8.4-8.7$) B2 V-IIIe star. Spectroscopic observations on 1994 February 13 show prominent Balmer emission with $EW(H\alpha) = -32 \text{ \AA}$. The GSC star nearest ($29''$) to the B star (GSC 0683600952; $V \approx 12.4$) but located slightly outside the 90% confidence survey error circle was also observed at this occasion and failed to reveal the signature characteristic of an active corona.

The source was detected again during a short dedicated PSPC pointing with a count rate about half of that recorded during the survey. The position resulting from the pointed observation is now only $6''$ away from HD 161103 and the energy distribution is clearly hard ($HR2 = +0.47 \pm 0.21$) although we still have too few photons to really characterize the energy distribution. The L_X/L_{bol} ratio is close to the end of the observed distribution for O stars (Sciortino et al. 1990). However, this is still ≈ 50 times more than for the B1-B2 type stars measured by Cassinelli et al. (1994). The corresponding un-absorbed 0.1-2.4 keV X-ray luminosities are close to $10^{32} \text{ erg s}^{-1}$.

Our conclusion is that the evidences in favour of an accreting component are strong but not firm enough in order to definitively claim that HD 161103 is a new Be/X-ray system. However, this object is a good candidate and would certainly deserve follow-up X-ray observations in a harder X-ray band.

5.1.7. SAO 49725 (Group 3)

SAO 49725 is a relatively bright B0e star ($V = 9.23$) suffering a reddening $E(B-V) \approx 0.67$. The survey source was recovered in a subsequent pointing with a count rate of about twice of that given by the EXSAS analysis for the survey. Both survey and pointed positions encompass SAO 49725 (see Fig. 19).

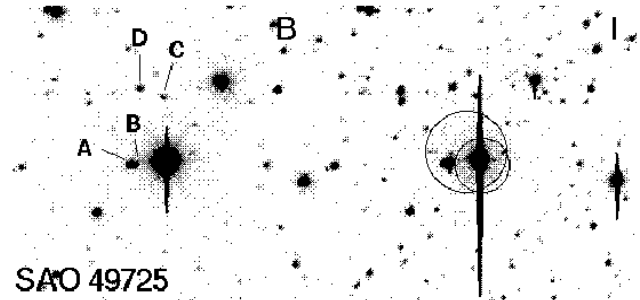


Fig. 19. B and I CCD images of the field of SAO 49725 obtained on 1992 May 27 with the CCD camera at the OHP 1.2 m telescope. Both images have 10 min exposure time. North is at top and East to the left. Each frame is 3.54×3.54 wide. On the I image we plot the ROSAT survey and pointed 90% confidence error circles. On the B band image we show the position of the other possible optical candidates which were spectroscopically investigated

None of the red excess candidates located in or close to the X-ray error circles and marked on Fig. 19 display any signature of chromospheric activity. Objects A, D and C are late G-F stars. Object B is a M star without any detectable Balmer or Ca II emission and is therefore an unlikely optical counterpart. Our blue medium resolution spectrum (see Fig. 20) displays, in addition to $H\beta$, O II,

C III and weak He II lines which indicate a B0.5 type in agreement with former determinations. The relative strength of the He II λ 4686 and He I λ 4713 and that of the Si II lines suggests a dwarf or giant luminosity class.

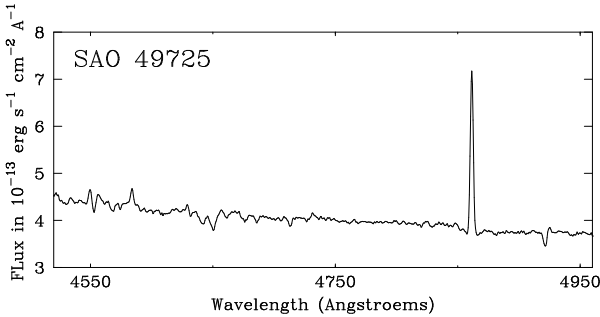


Fig. 20. Blue medium resolution spectrum of SAO 49725 obtained on 1992 October 22 at OHP with the 1.93 m telescope and the CARELEC spectrograph. Exposure time is 20 min

Fig. 21 shows the prominent H α (EW = $-30 \pm 1 \text{ \AA}$) and H β (EW = $-2.0 \pm 0.1 \text{ \AA}$) emission lines. The Balmer continuum is also seen in emission revealing the presence of a large circumstellar envelope.

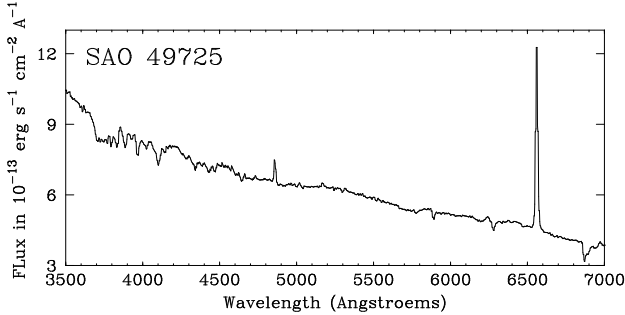


Fig. 21. Low resolution spectrum of SAO 49725 obtained on 1991 June 8 at OHP with the 1.93 m telescope and the CARELEC spectrograph. The 60% flux difference between this spectrum and that shown in Fig. 20 is due to inaccurate flux calibration. Exposure time is 2 min

The pointing data show that the X-ray source is relatively hard. With the updated optical and X-ray data, the L_X/L_{bol} ratio remains close to $3 \cdot 10^{-6}$. This is rather strong evidence, although not fully compelling, for an accreting compact object around SAO 49725.

5.2. Uncertain cases

HD 38087 (Group 1) : HD 38087 is a B5V star (Schild & Chaffee 1971) located in the Orion OB1 association. The distance resulting from the photometry is 470 pc in agreement with that derived by Warren & Hesser (1978)

for the belt subregion (~ 440 pc). However, the star is associated with a reflection nebulosity and may have an anomalous reddening law ($R_V = A_V/E(B-V) = 5.3-5.7$; Whittet & van Breda 1980, Cardelli et al. 1989) possibly caused by unusually large grains (Snow & Witt 1989). These authors derive a total $N_H = 4.0 \pm 0.5 \cdot 10^{21} \text{ cm}^{-2}$ whereas with an observed $E(B-V) = 0.29$ the expected N_H should be $\approx 2.3 \cdot 10^{21} \text{ cm}^{-2}$.

The position of the source was covered by two ROSAT pointings and it was detected on each occasion with a mean count rate similar to that observed during survey observations. Survey and pointing spectra have rather soft HR2s usually not observed in OB/X-ray systems. The spectrum accumulated from WG900386 can be represented by a two temperature thin thermal Raymond Smith spectrum ($kT_1 = 0.28 \text{ keV}$; $kT_2 = 3.1 \text{ keV}$; $N_H = 3 \cdot 10^{21} \text{ cm}^{-2}$) typical for active coronae. Assuming a distance of 470 pc the un-absorbed 0.1-2.4 keV X-ray luminosity is $\approx 7 \cdot 10^{31} \text{ erg s}^{-1}$ (two temperature plasma), close to that computed by the automatic process. Such a high X-ray luminosity is sometimes observed during flaring states in the most active T Tauri stars (see e.g. Montmerle et al. 1983). With an estimated cluster age of $5 \cdot 10^6 \text{ yr}$ for the OB1 b1 group (Warren & Hesser 1978) and considering the softness of the source, the X-ray emission could still originate from a very active late type star physically linked to HD 38037. The emission line star LkHA 291 is apparently located well outside the ROSAT error circle as seen from the finding chart in Herbig and Kuhi (1963).

HD 53339 (Group 1) : This B3V star belongs to the Canis Major OB1 association located at a distance of ≈ 1150 pc (Claria 1974). It consists of a close pair separated by $1''.1$ and with a magnitude difference of 0.9^m . If the pair is physically linked, the faint component is a late B star with little intrinsic X-ray emission. The Einstein IPC did not detect X-ray emission from the region with an upper limit of $5 \cdot 10^{-3} \text{ cts s}^{-1}$ probably consistent with the PSPC count rate of $2.3 \cdot 10^{-2} \text{ cts s}^{-1}$. Hardness ratios are marred by large errors and compatible with both an active corona or a hard accreting source. At the time of writing this paper the AO-3 pointing data covering HD 53339 were not available from the archive.

Our optical observations failed to reveal any alternative bright optical counterpart. However, several faint stars in the error circle (see Fig. 22) would deserve further investigation before settling the case. The reddish object B is a late K-M star without H α emission. With an estimated un-absorbed 0.1-2.4 keV X-ray luminosity of $\approx 6.5 \cdot 10^{31} \text{ erg s}^{-1}$ (computed using the results of the EXSAS analysis of the survey), HD 53339 clearly deserves further optical and X-ray monitoring.

HR 2875 (Group 1) : HR 2875 is a bright ($V = 5.41$) B5Vp star also detected by the ROSAT Wide Field Camera (Pounds et al. 1993). The PSPC energy distribution is extremely soft and therefore the standard process computing the L_X/L_{bol} ratio, which assumed a 10^7 K thin ther-

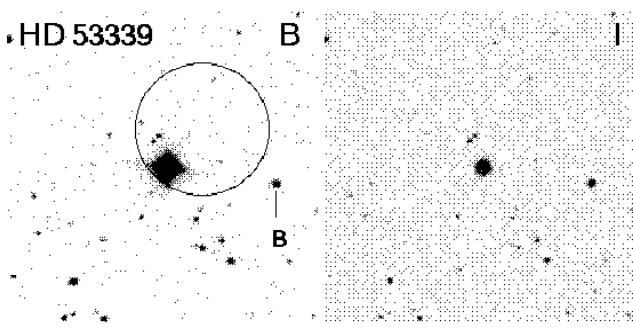


Fig. 22. B and I CCD images of the field of HD 53339 obtained on 1992 April 22 with EFOSC2 and the ESO-MPI 2.2 m telescope. Both images have 5 min exposure time. North is at top and East to the left. Each frame is 2.83×2.83 wide. On the B image we plot the ROSAT survey 90% confidence error circle and show the position of a late K-M star which we have investigated spectroscopically and which does not exhibit H α emission

mal emission, largely overestimated the X-ray flux in that particular case. No photon is detected above 350 eV in the ROSAT survey data and the overall PSPC spectrum looks like that of an isolated hot white dwarf. Considering the very low probability of a positional coincidence with such a bright star, the hypothetical white dwarf should be physically linked to the B5 star and at a distance of 190 pc the observed count rate is compatible with this hypothesis (see e.g. Barstow et al. 1994). The expected ‘normal’ harder X-ray emission from the early type star should give a count rate ≈ 200 times smaller than observed and virtually be undetectable in our data.

LS IV -12 70 (Group 1) : A source located at a position consistent with that found in the survey was re-detected during the PSPC pointing WG 500040. However, the pointed position is incompatible with the B star and a red excess object now lies in the middle of the revised error circle.

HD 38023 (Group 2) : This position was not optically investigated. The B4V star HD 38023 is located in Orion inside a reflection nebula. The X-ray source was detected again during a long PSPC pointing with a count rate similar to that recorded during the survey. HD 38023 now falls within the 90% confidence radius of the pointed position. It appears as the brightest spot of a patch of several nearby sources. RX J0542.3–0807 is variable between 0.01 and 0.04 cts s $^{-1}$ on a time scale of two days and displays a soft energy distribution. Fixing the interstellar absorption to the value derived from the optical colours ($N_{\text{H}} = 3.7 \times 10^{21} \text{ cm}^{-2}$) a thin thermal Raymond-Smith spectrum fit yields $kT = 0.85 \pm 0.12 \text{ keV}$ indicating that the PSPC energy distribution is compatible with that expected from an active corona. The corresponding mean un-absorbed 0.1–2.4 keV X-ray luminosity of $\approx 1.7 \times 10^{31} \text{ erg s}^{-1}$ is consistent with the luminosities derived by running the automatic

process on survey data. Considering the X-ray luminosity and softness of the source the odds are more in favour of a young late type star physically related to HD 38023 rather than for a genuine accreting binary.

LS V +29 14 (Group 2) : This position was not optically investigated. Comparison of POSS O and E plates reveals the presence close to the survey X-ray position of at least two faint red candidates which could be Me stars.

LS 5038 (Group 2) : The field of LS 5038 was covered by a long PSPC pointed observation. A weak source ($1.8 \times 10^{-3} \text{ cts s}^{-1}$, i.e. about 10 times fainter than the survey count rate) is detected at a position probably compatible with the survey position. The source detected during the pointing is now farther away ($93''$) from LS 5038 than was the survey position ruling out an association with the early type star. The pointed position is closer ($69''$) to the bright ($V = 8.0$) K0IV star HD 169651, however, the late type star is still outside the 90% confidence radius. Our optical spectroscopic observations failed to identify any active corona in the close neighbourhood of the early type star and revealed that LS 5038 is a Be star ($\text{EW}(\text{H}\alpha) = -4.4 \pm 0.3 \text{ \AA}$) exhibiting a central H α absorption core similar to that seen in LS 1698 and LS 992. The $\lambda 6284$ interstellar band indicates $E(\text{B-V}) \approx 0.85$. Our low resolution spectroscopic data do not allow accurate spectral type determination. We cannot completely rule out the unlikely possibility that we have witnessed a hard X-ray flare from an accreting object around LS 5038 during the survey observation.

HD 36262 (Group 3) : HD 36262 is another early type star in Orion displaying an X-ray excess. With a B3V spectral type and an un-absorbed X-ray luminosity of $3 \times 10^{31} \text{ erg s}^{-1}$ (using EXSAS results), the most likely explanation of the X-ray excess is the presence of an extremely active companion star. The hardness ratios are compatible with a rather soft stellar source.

5.3. Likely non-accreting sources

5.3.1. LS III +46 11 (Group 1)

This OB star is a probable member of the Berkeley 90 cluster (Sanduleak 1974) and located within the HII region Sharpless 115 (Harten & Felli 1980). LS III +46 11 is well placed within the ROSAT survey error circle. Spectroscopic observations of all nearby objects marked on Fig. 23 failed to reveal any convincing alternative optical counterpart leaving the OB star as the most likely identification of RX J2035.2+4651.

Medium resolution ($\lambda\lambda 3900\text{--}4400 \text{ \AA}$; Fig. 24 and $\lambda\lambda 6300\text{--}6700 \text{ \AA}$; Fig. 25) and low resolution ($\lambda\lambda 3800\text{--}7100 \text{ \AA}$; not shown) optical spectroscopy indicate a very hot giant star. The He II $\lambda 4541$ / He I $\lambda 4471$ and the He II $\lambda 4025$ / He II $\lambda 4200$ line ratios both indicate an O3–O5 spectral type (see Fig. 24). The probable presence of N IV $\lambda 4058$ emission also visible in our low resolution

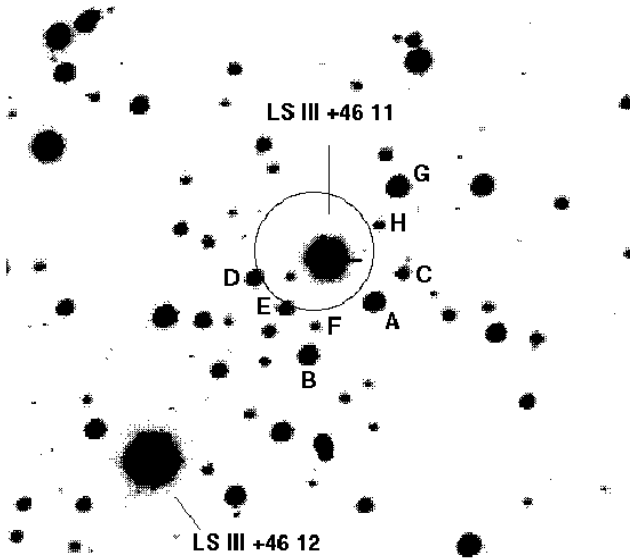


Fig. 23. B CCD image of the field of LS III +46 11 obtained on 1992 May 27 with the RCA3 CCD camera and the 1.2 m telescope at OHP. We show the 90% confidence ROSAT survey error circle and the position of the alternative candidate stars for which we obtained optical spectroscopy. North is at top and East to the left. The field is 3.54×3.54 wide

tion spectrum and possible N V λ 4606-4620 absorption suggest a class III luminosity. Broad H α emission is conspicuous and indicative of the high luminosity of the star (see Fig. 25). We thus propose an O3-O5III(f)e spectral type for LS III +46 11.

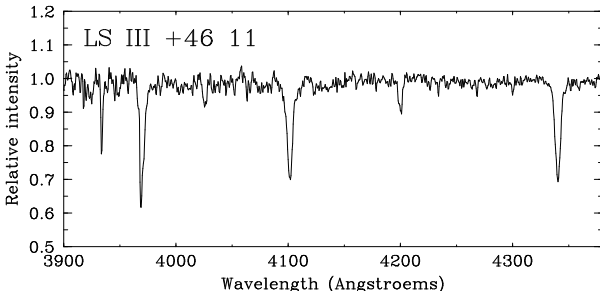


Fig. 24. Rectified blue medium resolution spectrum of LS III +46 11 obtained with the OHP 1.93 m telescope and the CARELEC spectrograph. The spectrum shown here is the mean of 4 spectra collected in the time interval 1991 November 20-24. Total exposure time is 100 min

In a subsequent dedicated pointed observation LS III +46 11 was again detected with a count rate consistent with that recorded during the survey (0.046 cts s^{-1}). The nearby O6 star LS III +46 12 was also detected with a count rate of $0.016 \pm 0.004 \text{ cts s}^{-1}$.

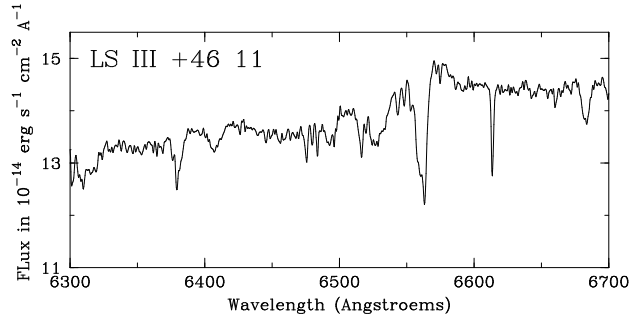


Fig. 25. Red medium resolution spectrum of LS III +46 11 obtained with the OHP 1.93 m telescope and the CARELEC spectrograph on 1992 December 15. A broad H α component ($\text{FWHM} \approx 60 \text{ \AA}$) is visible and indicative of the high stellar luminosity

In this particular case, the assumption of a default B0 III spectral type by the automatic SIMBAD/ROSAT correlation process led to a clear overestimation of the L_X/L_{bol} ratio. Using an O3 III spectral type now gives $L_X/L_{\text{bol}} \approx 2.7 \cdot 10^{-6}$. With this spectral type the star is at 1.9 kpc, in agreement with the distance of the Be 90 cluster and the 0.1-2.4 keV un-absorbed luminosity is of the order of $5 \cdot 10^{33} \text{ erg s}^{-1}$. We also note that the ratio of the PSPC count rate from LS III +46 11 over that of LS III +46 12 is similar to the ratio of their bolometric luminosities. This implies that most of the ionizing power in S 115 is actually provided by LS III +46 11 rather than by LS III +46 12. Although extremely rare, such high X-ray to bolometric ratios and soft X-ray luminosities have been reported for a few O type stars (Sciortino et al. 1990). We therefore conclude that there is probably no need for an accreting component in order to explain the X-ray emission of LS + 46 11. However, considering the extreme value of the X-ray luminosity this star would certainly deserve further detailed investigation.

5.3.2. Other sources

HD 59364 (Group 1): RX J0728.6-2629 is probably identified with a red Me star (object C in Fig. 26) which exhibits strong Ca II H&K emission and Balmer emission.

HD 67785 (Group 1): RX J0807.2-5053 is most likely identified with object "B" (see Fig. 27). This late K-M star displays Ca II H&K emission consistent with the X-ray flux.

HD 165424 (Group 1): Follow-up pointed PSPC observations give an improved position only $3''$ away from the $V = 9.0$ K0 star HD 315203 and the former proposed B4II identification HD 165424 is now outside the ROSAT error circle. Systematic attitude errors are unlikely to be large for this pointing since we detect the X-ray emission of the symbiotic star He 3 -1591 only $10''$ away from the opti-

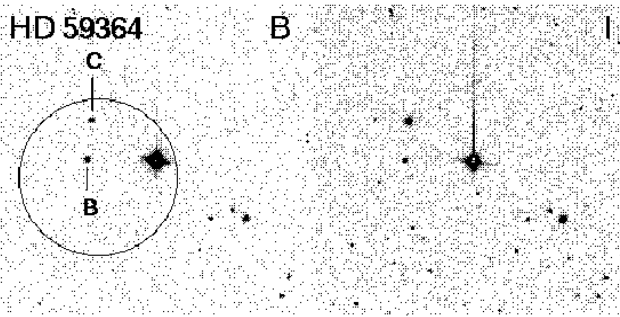


Fig. 26. B and I CCD images of the field of HD 59364 obtained on 1992 April 18 with EFOSC2 and the ESO-MPI 2.2 m telescope. Both images have 2 min exposure time. North is at top and East to the left. Each frame is 2.83×2.83 wide. On the B image we plot the ROSAT survey 90% confidence error circle and show the position of the objects investigated spectroscopically. We identify the X-ray source with the red Me star C

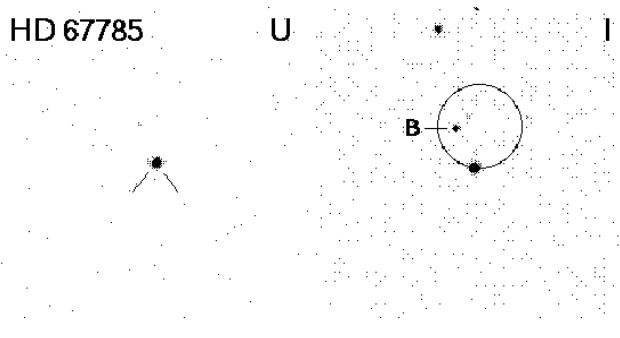


Fig. 27. U and I CCD images of the field of HD 67785 obtained on 1992 April 17 with EFOSC2 and the ESO-MPI 2.2 m telescope. Both images have 30 s exposure time. North is at top and East to the left. Each frame is 2.83×2.83 wide. On the U image we show the position of HD 67785. On the I image we plot the ROSAT survey 90% confidence error circle and show the position of object B which is the actual optical counterpart of RX J0807.2–5053

cal position. We conclude that RX J1806.8–2606 should rather be identified with the late type star HD 315203.

BD + 60 282 (Group 2) : RX J0136.7+6125 is probably identified with the $V = 10.7$ star GSC 0403100953, $10''$ away from the ROSAT survey position. Optical spectroscopy shows that GSC 0403100953 is a late type star displaying strong Ca II H&K emission consistent with the measured X-ray flux.

LS I +61 298 (Group 2) : RX J0234.4+6147 is probably identified with the $V = 14.1$ red excess object (GSC 0404700465) located $10''$ away from the survey position. Red medium resolution spectroscopy reveals the presence of narrow H α emission superposed on a deep absorption profile indicating that GSC 0404700465 is a late F or G type active star. The source was detected again during

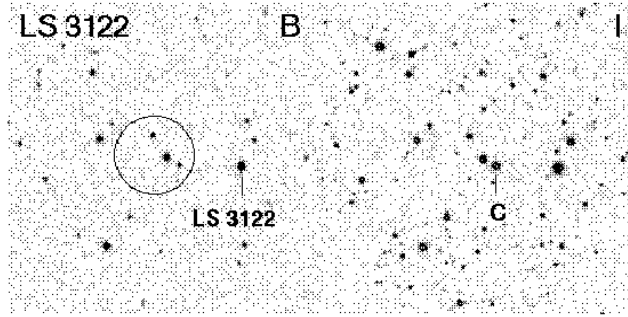


Fig. 28. B and I CCD images of the field of LS 3122 obtained on 1992 April 17 with EFOSC2 and the ESO-MPI 2.2 m telescope. Both images have 2 min exposure time. North is at top and East to the left. Each frame is 2.83×2.83 wide. On the B image we plot the ROSAT survey 90% confidence error circle and show the position of LS 3122. On the I band image we show the position of object C, the Me star optical counterpart of RX J1335.5–6211

an AO3 pointing with a count rate similar to that of the survey observation. The pointed position is closer to the B star ($19''$) but still compatible with the emission line candidate star ($34''$).

LS 3122 (Group 2) : The Me star (object C in Fig. 28) is the likely counterpart of RX J1335.5–6211. The star is located well inside the 90% confidence error circle and medium resolution red spectroscopy revealed strong H α emission ($EW \approx 6.0 \text{ \AA}$).

SS 73 49 (Group 2) : The emission line star Wray 15-1400 = SS 73 49 was discovered by Wray (1966) and is identified with GSC 0784600316. Using objective prism low resolution spectra Sanduleak & Stephenson (1973) classify the object as a Be type star. Our medium (Fig. 29) and low resolution (Fig. 30) spectra show strong Balmer and Ca II H&K emission. We classify SS 73 49 as a strong line T Tauri star rather than Be. Ca II H&K emission is unusual in Be stars and there are evidences for Mg b and TiO $\lambda\lambda 6187$ - 6215 bands in absorption suggesting a late K star underlying continuum. The Ca II H&K flux is consistent with that expected from the PSPC count rate for active coronae. The survey hardness ratios are also compatible with those normally observed from young active stars. Interactive analysis of the survey photons yields a position slightly closer to the active star at the edge of the 95% confidence error circle. We conclude that RX J1559.2–4157 is optically identified with the T Tauri star SS 73 49.

LS IV -05 35 (Group 2) : RX J1900.7–0503 is most probably identified with the $V = 12.2$ star GSC 0513601711 located within the 90% confidence error circle. Optical spectroscopy reveals noticeable Ca II H&K emission from GSC 0513601711.

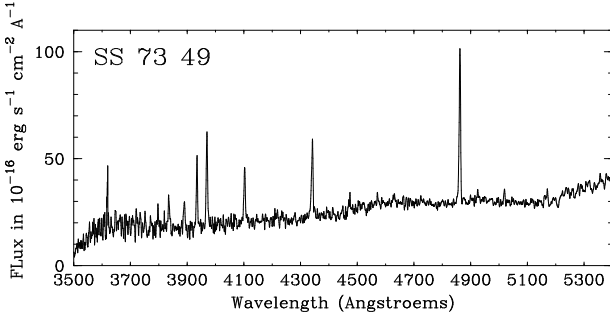


Fig. 29. Flux calibrated blue medium resolution spectrum of SS 73 49, the proposed optical counterpart of RX J1559.2–4157. The spectrum was obtained on 1992 April 20 with EFOSC2 and the ESO-MPI 2.2 m telescope. Exposure time is 10 min

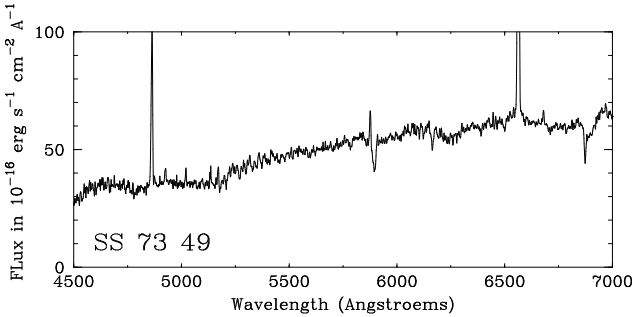


Fig. 30. Flux calibrated low resolution spectrum of SS 73 49, the proposed optical counterpart of RX J1559.2–4157. The spectrum was obtained on 1992 April 20 with EFOSC2 and the ESO-MPI 2.2 m telescope. Exposure time is 5 min

6. Discussion

We summarize in Table 8 the final list of identifications for all 24 sources resulting from our follow-up optical/X-ray studies. Spectral types were updated using our own determinations. In total we have discovered 5 very likely new massive X-ray binaries with an additional 2 good candidates needing further confirmation. Table 9 lists the main optical and X-ray characteristics of the 7 new massive X-ray binary candidates. Distances, X-ray luminosity and luminosity ratios are subject to various sources of error such as count rate statistics and unknown X-ray energy distribution, inaccuracies in the interstellar absorption and absolute photometric calibrations. A typical error of 25% to 50% on all three quantities is probably realistic. The same errors apply to data listed in Table 10.

6.1. Interlopers

The cross-correlation in position of large catalogues with the unprecedented number of sources present in the ROSAT all-sky survey unavoidably leads to numerous spurious matches. Further selection of associations with ex-

treme X-ray versus optical characteristics such as the one performed here enhances the fraction of wrong identifications and our present study clearly illustrates the need to ensure identification using X-ray and especially optical follow-up observations.

Several points of interest concerning the statistics of positional coincidence may be noted. First, all but 4 sources have a confirmed or a likely alternative optical counterpart within the 90% confidence radius. Among the 8 OB/X-ray associations outside the SASS 95% confidence radius (group 2) only one, SS 73 49 is confirmed. These evidences demonstrate the reliability of the survey ROSAT XRT positions and show that the centering statistics is well enough understood at least phenomenologically to be used as a constraining tool for systematic optical identification. Second, 3 sources listed in group 1 have a confirmed alternative optical counterpart physically unrelated to the OB star. A fourth case may be that of LS IV -12 70. This rate would be close to the number of spurious matches within the 95% confidence error radius that was estimated in Section 2.5 on the basis of the size of the cross-correlated samples. These three to four cases do appear in the first group consistent with the expectation in Section 2.5 that spurious associations will be preferentially found among the high L_X/L_{bol} objects. However, since similar comprehensive optical follow-up has not been carried out for the remainder of the 108 OB/X-ray associations no definite conclusions about the validity of the estimates for spurious matches can be drawn.

6.2. Comparison with previously known OB/X-ray binaries

Among the 13 massive X-ray binaries known before the launch of ROSAT and detected by the SASS analysis in the galactic plane survey, there are 8 Be/X-ray systems and 5 disk-fed or supergiant wind-fed binaries (see Table 10). Most of the detected pre-ROSAT Be/X-ray systems are transient sources and apart from EXO 2030+375 which was probably caught in weak outburst (Mavromatakis 1994) all other systems have X-ray luminosities typical of the quiescent state ($L_X = 5 \cdot 10^{33} - 5 \cdot 10^{34} \text{ erg s}^{-1}$ in the energy range 0.1–2.4 keV and corrected for photoelectric absorption).

The distribution in optical spectral types of the 7 new massive X-ray binary candidates compares well with that of the previously known systems. In particular, we do not find accreting candidates with spectral types later than B2 and having X-ray luminosities above $10^{32} \text{ erg s}^{-1}$ among the candidates earlier than B6, although the possibility to detect an excess of X-ray luminosity is in principle larger for the later stars. The absence of good accreting candidates later than B2 is also not an artifact of our selection criteria since our threshold of $L_X/L_{bol} = 3 \cdot 10^{-6}$ implies a limiting L_X of $\approx 10^{31} \text{ erg s}^{-1}$ at B5V and $7 \cdot 10^{31} \text{ erg s}^{-1}$ at B2V. In fact we do detect an excess of X-ray emission

Table 8. Summary of optical identifications. A.C. stands for active coronae. Spectral types are from our own determination or from the literature. Horizontal lines divide the three groups of candidates defined in Table 4

OB target Candidate	ROSAT Source Name	Optical Counterpart	Nature	Spectral Type
LS I +61 235	RX J0146.9+6121	LS I +61 235	Be/X	B1IIIe
BSD 24- 491	RX J0440.9+4431	BSD 24- 491	Be/X	B0V-IIIe
HD 38087	RX J0542.9-0218	HD 38087 ??	A.C. ??	
HD 53339	RX J0704.2-1123	HD 53339 ??	A.C. ??	
HD 59364	RX J0728.6-2629	Object C	A.C.	Me
HR 2875	RX J0729.0-3848	HR 2875 + WD ??	WD ??	
HD 67785	RX J0807.2-5053	Object B	A.C.	K-M
LS 992	RX J0812.4-3114	LS 992	Be/X	B0.5V-IIIe
LS 1698	RX J1037.5-5647	LS 1698	Be/X	B0V-IIIe
HD 165424	RX J1806.8-2606	HD 315203	A.C.	K0V
LS 5039	RX J1826.2-1450	LS 5039	OB/X	O7V((f))
LS IV -12 70	RX J1830.7-1232	??	A.C. ??	
LS III +46 11	RX J2035.2+4651	LS III +46 11	'Normal' O	O3-O5 III(f)e
BD +60 282	RX J0136.7+6125	GSC 0403100953	A.C.	G-K
LS I +61 298	RX J0234.4+6147	GSC 0404700456	A.C.	F-G ?
HD 38023	RX J0542.3-0807	HD 38023 ??	A.C. ??	
LS V +29 14	RX J0553.0+2939	??	??	
LS 3122	RX J1335.5-6211	Object C	A.C.	Me
SS 73 49	RX J1559.2-4157	SS 73 49	A.C.	T Tau
LS 5038	RX J1826.1-1321	??	??	
LS IV -05 35	RX J1900.7-0503	GSC 0513601711	A.C.	K-M
HD 36262	RX J0531.0+1206	HD 36262 ??	A.C. ??	
HD 161103	RX J1744.7-2713	HD 161103	Be/X ??	B2 V-IIIe
SAO 49725	RX J2030.5+4751	SAO 49725	Be/X ??	B0.5V-IIIe

Table 9. Optical and X-ray characteristics of the new OB/X-ray candidate systems. In this table we use the revised spectral types derived from our optical observations and the maximum X-ray count rates measured from survey or pointed PSPC observations and extracted using EXSAS. The last column lists the ratio of the maximum to minimum count rate observed between survey and pointed observations when significant variability is detected. The first five objects can be considered as very good OB/X-ray candidates whereas the last two require final confirmation of their X-ray excess

Optical Name	Spectral Type	V	B-V	U-B	E(B-V)	EW $\text{H}\alpha$ (Å)	d (kpc)	L_X/L_{bol}	L_X (erg s^{-1})	X-ray Variability
LS I +61 235	B1IIIe	11.33	0.82	-0.39	1.09	-7 -10	2.9	$2.7 \cdot 10^{-4}$	$2.7 \cdot 10^{34}$	1.8
BSD 24- 491	B0V-IIIe	10.78	0.61	-0.36	0.90	-2	3.2	$2.2 \cdot 10^{-5}$	$6.0 \cdot 10^{33}$	2.5
LS 992	B0.5V-IIIe	12.42	0.41	-0.69	0.70	-4.8	9.2	$7.0 \cdot 10^{-4}$	$1.3 \cdot 10^{35}$	≥ 95
LS 1698	B0V-IIIe	11.3			≈ 0.75	-1.5	5.0	$3.9 \cdot 10^{-5}$	$1.1 \cdot 10^{34}$	20
LS 5039	O7V((f))	11.23	0.94	-0.16	1.26	+2.7	3.1	$1.0 \cdot 10^{-5}$	$8.1 \cdot 10^{33}$	-
HD 161103	B2V-IIIe	8.4-8.7	0.44	-0.64	0.69	-32	0.8	$4.5 \cdot 10^{-6}$	$1.0 \cdot 10^{32}$	-
SAO 49725	B0.5V-IIIe	9.23	0.38	-0.65	0.67	-30	2.2	$2.6 \cdot 10^{-6}$	$5.0 \cdot 10^{32}$	-

in the range of $2\text{-}7 \cdot 10^{31} \text{ erg s}^{-1}$ from four B3V-B5V stars (HD 38087, HD 38023, HD 36262 and HD 53339). The youth of the OB associations in which these four extreme stars are located favours an explanation in terms of X-ray activity from a pre-main sequence low mass companion.

The distribution in X-ray luminosities of the four best Be/X-ray candidates is also comparable with that of known Be/X-ray systems in quiescence. On the other hand, the two additional candidates, HD 161103 and SAO 49725 have significantly lower X-ray luminosities.

The un-absorbed X-ray luminosities of the five first rank candidates clearly indicate that the accreting object

is a neutron star or less probably a black hole. All five sources have $\text{HR2} \geq 0.5$ similar to that exhibited by the majority of the known X-ray binaries, probably reflecting the hard intrinsic energy distribution. Unfortunately, in all cases, at most ≈ 100 photons were collected from the new sources preventing more detailed spectral modelling. Binary stellar evolution models predict the existence of five times more Be + white dwarf than Be + neutron star binaries (Pols et al. 1991). Waters et al. (1989) compute that white dwarfs accreting from a Be envelope should display X-ray luminosities in the range from 10^{29} to $10^{33} \text{ erg s}^{-1}$. So far there is no established Be + white dwarf

systems. Using ROSAT PSPC observations Haberl (1995) argues that γ Cassiopeiae could well be an example of a white dwarf accreting from the dense circumstellar envelope of a Be star although the hard X-ray properties of the source are consistent with those of an accreting neutron star in a widely separated orbit (White et al. 1982; Waters 1989). In our sample, only HD 161103 and SAO 49725 have low enough X-ray luminosities to qualify as Be + white dwarf candidates if their X-ray luminosity excess is confirmed. It may be noted that these two candidates have large Balmer emission revealing the presence of a high density envelope. A white dwarf could easily accrete enough matter from such a dense circumstellar material in order to produce the $\approx 10^{32} \text{ erg s}^{-1}$ detected by ROSAT. The X-ray spectrum of an accreting white dwarf in a Be envelope may not be necessarily as hard as that of a neutron star (see discussion in Meurs et al. 1992).

Two quite different mechanisms may account for the huge variations in X-ray luminosities often observed in these binaries. First, the motion of the compact star along an eccentric orbit with a period of weeks or longer may produce periodic outbursts when the X-ray source crosses the densest parts of the envelope close to periastron. Second, most Be stars are optically variable and this variability has usually been attributed to dramatic changes in the size and density of the equatorially condensed circumstellar envelope responsible for the Balmer and infrared emission. This second mechanism may produce large variations of the X-ray luminosity whatever is the orbital phase.

Our sample of four first rank new Be/X-ray systems probably illustrates all these possible configurations. Although the time interval between the X-ray and optical observation may introduce some additional scatter, it may be significant that these four Be stars display H α equivalent widths smaller than those of the previously known sources exhibiting X-ray outbursts (e.g. A1118-61, A0535+26, EXO2030+375). This suggests that the weakness of the envelope could to some extent explain the low persistent X-ray luminosities of LS 992 ($L_x \leq 1.4 \cdot 10^{33} \text{ ergs}^{-1}$) and the absence of strong recorded outbursts from BSD 24-491. On the other hand the relatively weak H α emitting Be star LS 1698 had a recorded bright outburst in the early seventies indicating that some of our new Be/X-ray sources could be hard X-ray transients in the quiescent state. These sources may undergo an outburst on the occasion of a future ejection of matter in the circumstellar envelope. LS 992 may be a particular case since it exhibited a factor 100 variation between survey and pointed observations. Optical spectroscopy contemporaneous to the pointed low state observations shows relatively weak H α emission at the same level as 7 months before. We could have here a low peak X-ray luminosity outbursting system where the main mechanism for variability is orbital motion. During the follow-up pointed observations two among of our seven new candidate X-ray binaries (LS 992 and LS 1698) displayed a PSPC count rate below the de-

tection threshold of the survey. This illustrates the strong variability of these sources and the well known fact that any new X-ray survey leads to the discovery of new members of this class.

6.3. Hard X-ray emission

A soft thermal bremsstrahlung component with a luminosity of typically $10^{34} \text{ erg s}^{-1}$ is observed from massive X-ray binaries with a supergiant counterpart (Haberl et al. 1994). This emission arises probably in a bow shock around the neutron star traveling through the dense stellar wind of the star. The X-ray luminosity of LS 5039 observed by ROSAT might be fully accounted for by this thermal emission. Also the hardness ratios are consistent with the values found for Vela X-1 from a pointed ROSAT observation ($HR1 = 0.99 \pm 0.01$ and $HR2 = 0.62 \pm 0.01$). The relation between X-ray luminosity in the thermal component and the luminosity in the hard spectrum originating at the neutron star strongly depends on the wind density and the system parameters and it is therefore difficult to predict the luminosity at higher energies.

Be/X-ray binaries on the other hand rarely show a soft component. For instance, the X-ray spectrum from X Persei is well represented by a power law with exponential high-energy cutoff between 0.1 and 12 keV as the combined ROSAT and BBXRT results show (Haberl 1994). For these systems the spectra might be extrapolated to higher energies, however the cutoff energy lies in general outside the ROSAT band and is not known.

A mean colour excess of $E(B-V) = 1.0$ for the new OB/X-ray binaries corresponds to $N_H = 5.5 \cdot 10^{21} \text{ cm}^{-2}$ (Predehl & Schmitt 1995). Assuming a power law spectrum with a photon index in the range of 0 - 2 and a cutoff energy $\geq 10 \text{ keV}$ (White et al. 1983, Tanaka 1986) implies that 1 PSPC count s^{-1} corresponds to an absorbed 2-10 keV flux in the range of $4 \cdot 10^{-11} - 7 \cdot 10^{-10} \text{ erg cm}^{-2} \text{ s}^{-1}$ or $\approx 2\text{-}30$ Uhuru count s^{-1} (Forman et al. 1978). The presence of a soft component will obviously decrease the hard X-ray flux corresponding to a given PSPC count rate. Therefore, with an estimated limiting count rate of ≈ 1 Uhuru count s^{-1} , highly depending on confusion effects in the galactic plane region, the new X-ray sources were most probably below the detection threshold of the all-sky surveys carried out by Uhuru and Ariel V (except for LS 1698 = 4U 1036-56 and LS I +61 235 which contributes to the Uhuru source 4U 0142+61). The absence of detection in the HEAO A-1 X-ray catalogue (Wood et al. 1984) above a 2-10 keV flux of $\approx 5 \cdot 10^{-12} \text{ erg cm}^{-2} \text{ s}^{-1}$ is also compatible with the recorded PSPC count rates.

6.4. Distribution of the new sources in the Galaxy

The distribution of the new massive X-ray binary candidates in the Galaxy follows the spiral arm structures traced by H II regions (Georgelin & Georgelin 1976) and

open clusters (Vogt & Moffat 1975). SAO 49725 and LS 992 are located on the local arm in opposite directions as seen from the Sun, BSD 24- 491 and LS I +61 235 are in the Perseus arm and LS 1698, HD 161103 and LS 5039 probably all belong to the Sagittarius-Carina arm. Comparing with optical absorption maps from Neckel & Klare (1980) shows that all new ROSAT detected massive X-ray binary candidates are in regions of relatively low interstellar absorption. This is not surprising considering the sensitivity of the PSPC count rate to interstellar extinction and the selection resulting from the correlation with optical catalogues. Stars with detailed spectral types are probably complete down to $B \approx 9$ -10 and the Luminous Star catalogue out of which about half of our optical input sample was extracted is complete down to $B \approx 12$. Therefore, the optical identifications reported here tend to be close to the completeness level of the optical input catalogue, clearly suggesting that several other systems with similar X-ray luminosities but without optical entries, because associated with fainter optical objects, may well be present in the ROSAT survey. This is consistent with the fact that among the 13 known massive X-ray binaries listed in Table 10, 5 had no known entries in optical catalogues before their X-ray discovery. In a future paper we will report on some of these new ROSAT discoveries.

In spite of the patchiness of interstellar absorption and incompleteness of the optical catalogues it may be possible to estimate the space density of massive X-ray binaries (see e.g. Meurs & van den Heuvel 1989) and the low end of their X-ray luminosity function using the ROSAT all-sky survey. Such a study may allow to constrain the contribution of this population to the overall hard X-ray emission of the Galaxy and more precisely to the hard X-ray galactic ridge detected by EXOSAT (Warwick et al. 1985).

7. Conclusions

Using the cross-correlation in position of the OB star catalogues held in SIMBAD with the low galactic latitude part of the RASS we selected 24 early type stars which apparently exhibited a soft X-ray excess over the normal stellar level. Follow-up optical and X-ray observations allowed to strongly suggest the presence of a compact object, probably a neutron star, in four cases and establish the X-ray binary nature of LS I +61 235. In two additional cases which still require confirmation the X-ray luminosity may be compatible with that expected from an accreting white dwarf.

The new massive X-ray binary candidates are clearly representative of the low end of the X-ray luminosity function. Their soft X-ray luminosities are comparable to those of hard X-ray transients in quiescence and those of the low luminosity Be/X-ray systems such as X Persei. One of the new Be/X-ray systems is the probable counterpart of 4U 1036-56 which was in outburst during the years 1970-1976.

Four B stars located in the Orion and Canis Major OB associations exhibit X-ray luminosities in the range of $2-7 \cdot 10^{31} \text{ erg s}^{-1}$ well above the expected normal stellar emission. Such X-ray luminosities appear at the high end of the luminosity distribution of active stars and the usual interpretation in terms of a young late type companion star may not hold.

Finally we report the probable discovery of a white dwarf companion to the B5V type star HR 2875.

Acknowledgements. We thank N. Fourniol, P. Guillout and the night assistants at Observatoire de Haute-Provence for carrying out some of the observations at the 1.2 m and 1.93 m telescope. We also thank S.A. Golçalves and R.D.A. da Costa for carrying out some of the observations at the 1.6 m of L.N.A. The ROSAT project is supported by the German Bundesministerium für Bildung, Wissenschaft, Forschung und Technologie (BMBF/DARA) and the Max-Planck-Gesellschaft. C.M. acknowledges support from a CNRS-MPG cooperation contract and thanks Prof. J. Trümper and the ROSAT group for their hospitality and fruitful discussions. We acknowledge detailed and useful comments from an anonymous referee. GSC data were extracted from the STARCAT facility at ESO (Pirenne et al. 1993) and later from the SIMBAD catalogue GSC browser (Preite-Martinez & Ochsenbein 1993). This research has made large use of the SIMBAD database operated at CDS, Strasbourg, France.

References

Apparao, K.M., 1994, *Space Science Reviews*, 69, 255
 Barstow, M.A., Holberg, J.B., Fleming, T.A., Marsh, M.C., Koester, D., Wonnacott, D., 1994, *MNRAS* 270, 499
 Berghöfer, T.W., Schmitt, J.H.M.M., 1994, *A&A* 292, L5
 Bigay, J.H., 1963, *J. Obs.*, 46, 319
 Bondi, H., Hoyle, F., 1944, *MNRAS* 104, 273
 Bromage, G.E., Nandy, K., 1973, *A&A* 26, 17
 Buckley, D.A., Tuohy, I.R., Remillard, R.A., 1985, *Proc. Astron. Soc. Australia*, 6, 147
 Buzzoni, B., Delabre, B., Dekker, H., D'Odorico, S., Enard, D., Focardi, P., Gustafson, B., Nees, W., Paureau, J., Reiss, R., 1984, *Messenger*, 38, 9
 Cardelli, J.A., Clayton, G.C., Mathis, J.S., 1989, *ApJ* 345, 245
 Cassinelli, J.P., Waldron, W.L., Sanders, W.T., Harnden, F.R., Jr, Rosner, R., Vaiana, G.S., 1981, *ApJ* 250, 677
 Cassinelli, J.P., Cohen, D.H., MacFarlane, J.J., Sanders, W.T., Welsh, B.Y. 1994, *ApJ* 421, 705
 Claria, J.J., 1974, *A&A* 37, 229
 Chlebowski, T., Harnden, F., Sciortino, S., 1989, *ApJ* 341, 427
 Coe, M.J., Everall, C., Norton, A.J., Roche, P., Unger, S.J., Fabregat, J., Reglero, V., Grunsfeld, J.M., 1993, *MNRAS* 261, 599
 Coyne, G.V., McConnell, D.J., 1983, *Vatican Obs. Publ.*, 1, part no 6, 73
 Deutschman, W.A., Davis, R.J., Schild, R., 1976, *ApJS* 30, 97
 Dennerl, K., 1991, PhD Thesis, Universität München, MPE Report 232
 Didelon, P., 1982, *A&AS* 50, 199
 Drilling, J.S., 1975, *AJ* 80, 128
 Fleming, T.A., Liebert, J., Gioia, I.M., Maccacaro, T., 1988, *ApJ* 331, 958

Table 10. Optical and X-ray characteristics of the known OB/X-ray systems detected by ROSAT during the all-sky survey at $|b| \leq 20^\circ$. About 5% of the galactic sky is not covered by this study (see Section 2.1). Distances, L_x/L_{bol} and L_x are computed using the automatic process described in section 2.4 and the results of the SASS analysis. The first group consists of Be/X-ray systems and the second group gathers disk and wind fed high mass X-ray binaries

Source Name	Spectral Type	EW(H α) range (Å)	d (kpc)	L_x/L_{bol}	L_x (erg s $^{-1}$)	HR1	HR2
LS 437 = A0726-260	B0-1e	-5.5	8.0	$1.1 \cdot 10^{-4}$	$4.9 \cdot 10^{34}$	0.76 ± 0.16	0.45 ± 0.29
He 3 -640 = A1118-61	O9.5V-IVe	-50 -60	3.2	$1.8 \cdot 10^{-5}$	$5.4 \cdot 10^{33}$	0.62 ± 0.43	0.59 ± 0.46
1H1909+096	Be	-16	3.2	$1.7 \cdot 10^{-5}$	$2.5 \cdot 10^{34}$	0.87 ± 0.12	0.85 ± 0.14
EXO 2030+375	Be	-9 -15	5.6	$1.1 \cdot 10^{-3}$	$4.9 \cdot 10^{35}$	0.97 ± 0.03	0.95 ± 0.04
LS I +65 10 = 3A 0114+650	B0.5IIIe	-2.1	2.6	$5.2 \cdot 10^{-5}$	$1.7 \cdot 10^{34}$	1.00	0.82 ± 0.16
V615 Cas = 1E 0236.6+6100	B0.5V-IIIe		3.1	$4.4 \cdot 10^{-5}$	$2.0 \cdot 10^{34}$	0.66 ± 0.29	0.03 ± 0.71
HR 1209 = X Per	O9.5V-IIIe	0 -15	0.76	$1.7 \cdot 10^{-5}$	$9.1 \cdot 10^{33}$	0.96 ± 0.04	0.39 ± 0.03
HD 245770 = A 0535+26	O9.7Ve	-15 -20	2.7	$3.8 \cdot 10^{-5}$	$1.7 \cdot 10^{34}$	0.91 ± 0.09	0.34 ± 0.10
HD 226868 = Cyg X-1	O9.7Iab		2.3	$1.8 \cdot 10^{-3}$	$2.7 \cdot 10^{36}$	0.99 ± 0.01	0.47 ± 0.01
HD 77581 = Vela X-1	B0.5Ib		1.8	$1.8 \cdot 10^{-5}$	$2.7 \cdot 10^{34}$	1.00	0.64 ± 0.03
HD 153919 = 4U 1700-37	O6.5Iaf+		1.1	$5.4 \cdot 10^{-6}$	$6.0 \cdot 10^{33}$	0.97 ± 0.03	0.91 ± 0.03
Cen X-3	O6.5II-III		13.0	$1.0 \cdot 10^{-3}$	$1.1 \cdot 10^{36}$	0.91 ± 0.09	0.60 ± 0.11
V830 Cen = 1E1145.1-6141	B2Iae		4.5	$2.2 \cdot 10^{-4}$	$9.1 \cdot 10^{34}$	0.92 ± 0.08	0.80 ± 0.18

Forman, W., Jones, C., Cominsky, L., Julien, P., Murray, S., Peters, G., Tananbaum, H., Giacconi, R., 1978, ApJS 38, 357

Georgelin, Y.M., Georgelin, Y.P., 1976, A&A 49, 57

Griffiths, R.E., Padovani, P., 1990, ApJ 360, 483

Guillout, 1996, Ph.D. Thesis, Strasbourg University Louis Pasteur

Haberl, F., White N.E., Kallman T.R., 1989, ApJ 343, 409

Haberl, F., White, N.E., 1990, ApJ 361, 225

Haberl F., 1994, A&A 283, 175

Haberl, F., Aoki, T., Mavromatakis, F., 1994, A&A 288, 796

Haberl, F., 1995, A&A 296, 685

Hardop, J., Rohlfs, K., Slettebak, A., Stock, J., 1959, Hamburger Sternwarte-Warner and Swasey Obs., Hamburg-Bergedorf, Vol. I

Harten, R., Felli, M., 1980, A&A 89, 140

Hellier, C., 1994, MNRAS 271, L21

Herbig, G.H., Kuhu, L.V., 1963, ApJ 137, 398

Humphreys, R.M., McElroy, D., 1984, ApJ 284, 565

Israel, G.L., Mereghetti, S., Stella, L., 1994, ApJ 433, L25

Jaschek, C., Jaschek, M., 1987, "The Classification of stars", Cambridge University Press.

Johnson, H.L., 1966, Ann. Rev. Astr. and Ap., 3, 193

Krelowski, J., Walker, G.A.H., Grieve, G.R., Hill, G.M., 1987, ApJ 316, 449

Lasker, B.M., Sturch, C.R., McLean, B.J., Russel, J.L., Jenkner, H., Shara, M.M., 1990, AJ 99, 2019

Lemaitre, G., Kohler, D., Lacroix, D., Meunier, J.P., Vin, A., 1990, A&A 228, 546

Long, K.S., White, R.L., 1980, ApJ 239, L65

Lucy, L.B., White, R.L., 1980, ApJ 241, 300

McConnell, D.J., Coyne, G.V., 1983, Vatican Obs. Publ. 2, No. 5, 63

Maggio, A., Sciortino, S., Vaiana, G.S., Majer, P., Bookbinder, J., Golub, L., Harnden, F.R. Jr., Rosner, R., 1987, ApJ 315, 687

Markert, T.H., Winkler, P.F., Laird, F.N., Clark, G.W., Hearn, D.R., Sprott, G.F., Li, F.K., Bradt, H.V., Lewin, W.H.G., Schnopper, H.W., 1979, ApJS 39, 573

Mavromatakis, F., 1994, A&A 285, 209

Meurs, E.J.A., van den Heuvel, E.P.J., 1989, A&A 226, 88

Meurs, E.J.A., Piters, A.J.M., Pols, O.R., Waters, L.B.F.M., Cote, J., van Kerkwijk, M.H., van Paradijs, J., Burki G., Taylor, A.R., De Martino, D., 1992, A&A 265, L41

Micela, G., Sciortino, S., Vaiana, G.S., Harnden, F.R., Rosner, R., Schmitt, J.H.M.M., 1990, ApJ 348, 557

Montmerle, T., Koch-Miramond, L., Falgarone, E., Grindlay, J.E., 1983, ApJ 269, 182

Motch, C., Stella, L., Janot-Pacheco, E., Mouchet, M., 1991a, ApJ 369, 490

Motch, C., Belloni, T., Buckley, D., Gottwald, M., Hasinger, G., Pakull, M.W., Pietsch, W., Reinsch, K., Remillard, R.A., Schmitt, J.H.M.M., Trümper, J., Zimmermann, H.-U., 1991b, A&A 246, L24

Motch, C., Haberl, F., Guillout, P., Pakull, M.W., Reinsch, K., Krautter, J., 1996a, A&A 307, 459

Motch, C., Guillout, P., Haberl, F., Pakull, M.W., Pietsch, W., Reinsch, K., 1996b, A&A, in press

Motch, C., Pakull, M., Haberl, F., Dennerl, K., 1996c, IAU Circ No 6285

Motch, C., Haberl, F., Dennerl, K., Pakull, M.W., Janot-Pacheco, E., 1996d, MPE report 263, p 165

Neckel, Th., Klare, G., 1980, A&AS 42, 251

Neuhäuser, R., Sterzik, M.F., Schmitt, J.H.M.M., Wichmann, R., Krautter, J., 1995, A&A 297, 391

Olsen, E.H., 1994, A&AS 104, 429

Ottmann, R., Schmitt, J.H.M.M., 1992, A&A 256, 421

Pallavicini, R., Golub, L., Rosner, R., Vaiana, G.S., Ayres, T., Linsky, J.L., 1981, ApJ 248, 279

Pfeffermann, E., Briel, U.G., Hippmann, H., Kettenring, G., Metzner, G., Predehl, P., Reger, G., Stephan, K.H., Zombeck, M.V., Chappell, J., Murray, S.S., 1986, SPIE, 733, 519

Pirenne, B., Albrecht, M., Durand, D., Gaudet, S., 1993, "Astronomical Data Analysis Software and Systems II", Eds. Hanish R. J., Brissenden R. J. V., Barnes J., Astronomical Society of the Pacific, p.95,99

Pols, O.R., Coté, J., Waters, L.B.F.M., Heise, J., 1991, A&A 241, 419

Pounds et al., 1993, MNRAS 260, 77

Predehl, P., Schmitt, J.H.M.M., 1995, A&A 293, 889

Preite-Martinez, A., Ochsenbein, F., 1993, in Proceedings of the "ESO/OAT Workshop on Handling and Archiving Data from Ground-based Telescopes" (May 1993). Eds F. Pasian & M. Albrecht.

Raymond, J.C., Smith, B.H., 1977, ApJS 35, 419

Reed, B.C., 1990, AJ 100, 737

Rosner, R., Golub, L., Vaiana, G.S., 1985, ARA&A, 23, 413

Sanduleak, N., Stephenson, C.B., 1973, ApJ 185, 899

Sanduleak, N., 1974, PASP 86, 74

Schild, R.E., Chaffee, F., 1971, ApJ 169, 529

Schmitt, J.H.M.M., Golub, L., Harnden, F.R.Jr., Maxson, C.W., Rosner, R., Vaiana, G.S., 1985, ApJ 290, 307

Schmitt, J.H.M.M., Collura, A., Sciortino, S., Vaiana, G.S., Harnden, F.R., Rosner, R., 1990, ApJ 365, 704

Schmitt, J.H.M.M., Zinnecker, H., Crudace, R., Harnden, F.R., 1993, ApJ 402, L13

Sciortino, S., Vaiana, G.S., Harnden, F.R., Ramella, M., Mrossi, C., Rosner, R., Schmitt, J.H.H.M., 1990, ApJ 361, 621

Seyfert, C.K., Popper, D.M., 1941, ApJ 93, 461

Slettebak, A., Stock, J., 1957, Zeitschrift für Astrophysik, 42, 67

Slettebak, A., 1985, ApJS 59, 769

Snow, T., Witt, A., 1989, ApJ 342, 295

Stephenson, C.B., Sanduleak, N., 1971, Publ. Warner and Swasey Obs. 1, 100

Tanaka, Y., 1986, in "Radiation Hydrodynamics in Stars and Compact Objects", Eds D. Mihalas & K.-H.A. Winkler, p198

Tapia, M., Costero, R., Echevarria, J., Roth, M., 1991, MNRAS 253, 649

Trümper, J., 1983, Adv. Space Res., 2, 241

Turnshek, D.E., Turnshek, D.A., Craine, E.R., Boeshaar, P.C., 1985, "An Atlas of Digital Spectra of Cool Stars" Western Research Company, Astronomy & Astrophysics Series, Ed E.R. Craine.

Van den Heuvel, E.P.J., Rappaport, S., 1987, in "Physics of Be Stars", Proc. IAU Colloq. No. 92, Eds. Slettebak, A. and Snow, T.P. (Cambridge: Cambridge Univ. Press) p361

Verbunt, F., van den Heuvel, E.P.J., 1995, in "X-ray binaries" Eds. W.H.G. Lewin, E.P.J. van den Heuvel (Cambridge: Cambridge Univ. Press)

Voges, W., 1992, in Proceedings of Satellite Symposium 3, "International Space Year Conference", ESA ISY-3, p9

Voges, W., Gruber, R., Paul, J., Bickert, K., Bohnet, A., Burzik, J., Dennerl, K., Englhauser, J., Hartner, G., Jennert, W., Köhler, H., Rosso, C., 1992, in Proceedings of Satellite Symposium 3, "International Space Year Conference", ESA ISY-3, p1

Vogt, N., Moffat, A.F.J., 1975, A&A 39, 477

Walborn, N.R., 1973, AJ 78, 1067

Walborn, N., Fitzpatrick, E., 1990, PASP 102, 379

Waldron, W., 1984, ApJ 282, 256

Walter, F.M., Bowyer, C.S., 1981, ApJ 245, 671

Warren, W.H., Hesser, J.E., 1978, ApJS 36, 497

Warwick, R.S., Marshall, N., Fraser, G.W., Watson, M.G., Lawrence, A., Page, C.G., Pounds, K.A., Ricketts, M.J., Sims, M.R., Smith, A., 1981, MNRAS 197, 865

Warwick, R.S., Turner, M.J.L., Watson, M.G., Willingale, R., 1985, Nat 317, 218

Waters, L.B.F.M., Pols, O.R., Hogeveen, S.J., Coté, J., van den Heuvel, E.P.J., 1989, A&A 220, L1

Waters, L.B.F.M., 1989, Proc. 23 ESLAB Symposium, ESA SP-296, Vol 1., p.25

White, N.E., Swank, J.H., Holt, S.S., Parmar, A.N., 1982, ApJ 263, 277

White, N.E., Swank, J.H., Holt, S.S., 1983, ApJ 270, 711

Whittet, D.C.B., Van Breda, I.G., 1980, MNRAS 192, 467

Wood, K.S., Meekins, J.F., Yentis, D.J., Smathers, H.W., McNutt, D.P., Bleach, R.D., Byram, E.T., Chubb, T.A., Friedman, H., Meidav, M.J., 1984, ApJS 56, 507

Wray, J.D., 1966, Ph.D. Thesis, Northwestern University

Zimmermann, H.U., Belloni, T., Izzo, C., Kahabka, P., Schwenk, O., 1992, MPE Report 48